Effects of slip condition on the peristaltic flow of a non-Newtonian fluid

By

Raheel Ahmed

Supervised by

Dr. Nasir Ali

Department of Mathematics & Statistics
Faculty of Basic and Applied Sciences
International Islamic University, Islamabad
Pakistan, 2011

(1) Peristaltic flow of a non-newtonian

بسم الله الرحمن الرحيم

**In the name of Almighty ALLAH,
the most beneficent and the most merciful**

Effects of slip condition on the peristaltic flow of a non-Newtonian fluid

By

Raheel Ahmed

Department of Mathematics & Statistics
Faculty of Basic and Applied Sciences
International Islamic University, Islamabad
Pakistan, 2011

Effects of slip condition on the peristaltic flow of a non-Newtonian fluid

By

Raheel Ahmed

A Thesis
Submitted in the Partial Fulfillment of the
Requirements for the Degree of
MASTER OF SCIENCE
In
MATHEMATICS

Supervised by

Dr. Nasir Ali

Department of Mathematics & Statistics
Faculty of Basic and Applied Sciences
International Islamic University, Islamabad
Pakistan, 2011

Certificate

Effects of slip condition on the peristaltic flow of a non-Newtonian fluid

By

Raheel Ahmad

A DISSERTATION SUBMITTED IN THE PARTIAL FULFILLMENT OF THE REQUIREMENTS FOR THE DEGREE OF THE **MASTER OF SCIENCE IN MATHEMATICS**

We accept this dissertation as conforming to the required standard.

1. ______________________
Dr. Irshad Ahmad Arshad
(Chairman)

2. ______________________
Dr. Nasir Ali
(Supervisor)

3. ______________________
Prof. Dr. Nawazish Ali Shah
(External Examiner)

4. ______________________
Dr. Ahmad Zeeshan
(Internal Examiner)

Department of Mathematics & Statistics
Faculty of Basic & Applied Science
International Islamic University Islamabad,
Pakistan, 2011.

<u>Dedicated to</u>

My Father (Late), My Loving Mother and all family members, whose prayers are always a great source of motivation for me.

Declaration

I, hereby declare that this dissertation, neither as a whole nor as a part thereof, has been copied out from any source. It is further that I have prepared this dissertation entirely on the basses of my personal effort made under the sincere guidance of my supervisor. No portion of the work, presented in this dissertation, has been submitted in support of any application of any degree or qualification of this or any other university or institute of learning.

Signature: ______________

Raheel Ahmed
MS (Mathematics)
Registration No: 44-FBAS/MSMA/F09
Department of Mathematics and Statistics Faculty of Basic and Applied Sciences International Islamic University, Islamabad, Pakistan.

Acknowledgements

Foremost, I am always grateful to Almighty ALLAH, who made human being, the best creation of all the living species and made them understand to write with pen. He provided me the boldness and capability to achieve this task. I offer countless Darood and Salaams to my beloved Holy Prophet HAZRAT MUHAMMAD (PBUH), for whom this universe has been manifested. ALLAH has shown His existence and oneness by sending him as a messenger of Islam and born me as a Muslim.

I offer my most sincere gratitude to my affectionate, sincere, kind and most respected supervisor **Dr. Nasir Ali**, whose kinetic supervision, admonition in a right inclination and inductance of hard work made my task easy and I completed my dissertation well with in time. His ideology and concepts have a remarkable impact on my research contrivances. He also arranged some suitable facilities, without which my objective might not be attained. I have learnt a lot from his ability.

I am grateful to all of my teachers. They always guided me sincerely and honestly throughout my course work as well as research work.

I also offer special thanks to all my friends and my class fellows, who really helped me to their best throughout my research period. They helped me throughout my work, whenever I faced any difficulty relating my problem.

Raheel Ahmed

Preface

The study of flow dynamics of a fluid confined in a tube of a circular cross section, induced by a traveling wave on its wall, has tremendous application in science and engineering. The physical mechanism of the flow induced by the traveling wave can be well understood and in known as the so-called peristaltic transport mechanism. The motion of fluid in the body of living creatures is caused due to this mechanism. Such mechanism frequently occurs in organs such as ureter, intestines and arterioles. Peristaltic pumping is also involved in the functioning of medical instruments such as the heart-lung machine. Some recent investigations in this area can be found in refs. [1-10].

A literature survey reveals that usually peristaltic motion is analyzed with a motivation that it has application in physiology. In recent past it has been shown by the researchers [11, 12] that an external sonic radiation can considerably increases the flow rate of a liquid through a porous medium. Initially Ganiev and collaborates [13] performed the flow simulation via the wave travelling on the flow boundary in the context of porous media. They proposed that sonic radiation generates travelling waves on the pore walls in a porous medium. These waves in turn, generate a net flow of fluid via the peristaltic mechanism.

In all the above cited references the nature of the fluid was assumed to be Newtonian, however, e.g., oil and other hydrocarbons exhibit significant non-Newtonian behavior. Therefore some researchers extended the work presented for classical Newtonian fluid in ref. [11] for non-Newtonian fluids [14]. A further extension of the work done by Tsiklauri and Beresnev in [14] was made by El-Shehawy et al. [15]. They studied the peristaltic compressible flow of a Maxwellian fluid in a cylindrical pore by considering slip at the wall of the tube.

Motivated by the above mentioned studies, this dissertation extends the work presented in ref. [15] for a Jeffrey fluid. In fact the work conducted in the chapter 3 of this dissertation contains the previous studies [11, 14-16] as a special case. The brief layout of the dissertation is as follows.

Chapter 1 is introductory in nature and presents basic definitions and equations. Chapter 2 is a review of work by El-Shehawy et al. [15]. Missing mathematical details and all graphical results of ref. [15] are reproduced in this chapter. Peristaltic compressible flow of a Jeffrey fluid in the presence of slip at the wall is investigated in chapter 3. The effects of non-dimensional slip parameter, relaxation and retardation times on net flow rate are analyzed in detail. The dissertation ends up with a comprehensive bibliography.

Contents

Chapter 1

Preliminaries

The aim of this chapter is to provide some basic concepts and definitions which are to be used in the formulation of the problems in the next chapters.

1.1 Fluid

A fluid is a substance which continuously deforms under the application of shear stress.

1.2 Stress

Stress is defined as force per unit area acting on an infinitesimal surface element. Stress has both magnitude and direction, and the direction is relative to the surface on which stress acts. There are two type of stresses normal stress and tangential stress. The normal stress acts inwards that is towards the surface and is perpendicular to the surface, while the shear stress is the example of the tangential stress acts along the surface.

1.3 Pressure

Pressure is a force that acts normal to the area under consideration. Pressure is the example of normal stress. When a fluid is contained in a vessel, it exerts some force at each point of the inner surface. Such a force per unit are is known as pressure. The pressure p at a point is defined as

$$p = \lim_{\delta S \to 0} \left(\frac{\delta F}{\delta S} \right), \tag{1.1}$$

where δS is an elementary area and δF is the normal force due to fluid on δS.

1.4 Density

Density of the fluid is mass per unit volume. It is denoted by ρ and is given by

$$\rho = \frac{m}{V}. \tag{1.2}$$

In the above relation V is volume and m is mass the fluid within V.

1.5 Velocity

The velocity of a fluid is a vector field $\mathbf{v} = \mathbf{v}(x, y, z)$ which gives the velocity of an element of fluid at a position (x, y, z) and time t in components form we can write

$$\mathbf{v} = [u(x, y, z, t), v(x, y, z, t), w(x, y, z, t)]. \tag{1.3}$$

1.6 Viscosity

Viscosity is the fluid property by virtue of which a fluid offers resistance to shear stress. Newtons law of viscosity states that for a given rate of angular deformation of a fluid, shear stress is directly proportional to angular deformation. Viscosity at any point of the fluid is defined as

$$\mu = \frac{\tau_{xy}}{du/dy}, \tag{1.4}$$

where τ_{xy} denotes the shear stress acting in x -direction on the plane whose normal is in y-direction. du/dy is the rate of angular deformation and u is component of velocity in x-direciton.

1.7 Angular Deformation

Angular deformation of a fluid involves changes in angle between two mutually perpendicular lines.

1.8 Kinematic Viscosity

It is the ratio of dynamic viscosity to density. It is denoted by ν and is given by

$$\nu = \frac{\mu}{\rho}. \tag{1.5}$$

1.9 Strain Rate and Vorticity Tensors

The velocity gradient tensor $\nabla \mathbf{V}$ can be decomposed into a symmetric part $\mathbf{D}$ and antisymmetric part $\mathbf{W}$ as

$$\mathbf{D} = \frac{1}{2}\left(\nabla\mathbf{V} + \nabla\mathbf{V}^T\right) = \frac{1}{2}\dot{\gamma}, \tag{1.6}$$

$$\mathbf{W} = \frac{1}{2}\left(\nabla\mathbf{V} - \nabla\mathbf{V}^T\right) = \frac{1}{2}\omega, \tag{1.7}$$

where $\dot{\gamma}$ is called the rate of strain tensor and ω is called the vorticity tensor. Also it is noted that $\dot{\gamma} = \left(\nabla\mathbf{V} + \nabla\mathbf{V}^T\right)$ is equal to the Rivlin-Ericksen kinematic tensor. The vorticity is defined by

$$\omega = \nabla\mathbf{V} - \nabla\mathbf{V}^T = \nabla \times \mathbf{V}.$$

1.10 Gradient of Velocity

The gradient of velocity $\mathbf{V}$ is defined as

$$\nabla\mathbf{V} = \left(\mathbf{e}_j \frac{\partial}{\partial x_j}\right)\mathbf{V}_k\mathbf{e}_k = \mathbf{e}_j\mathbf{e}_k\frac{\partial \mathbf{V}_k}{\partial x_j}. \tag{1.8}$$

In a matrix form we can write

$$\nabla \mathbf{V} = \begin{bmatrix} \frac{\partial V_1}{\partial x_1} & \frac{\partial V_2}{\partial x_1} & \frac{\partial V_3}{\partial x_1} \\ \frac{\partial V_1}{\partial x_2} & \frac{\partial V_2}{\partial x_2} & \frac{\partial V_3}{\partial x_2} \\ \frac{\partial V_1}{\partial x_3} & \frac{\partial V_2}{\partial x_3} & \frac{\partial V_3}{\partial x_3} \end{bmatrix}. \tag{1.9}$$

1.11 Divergence of a Vector

The divergence of a vector is defined by

$$\nabla . \mathbf{V} = \left(\mathbf{e}_j \frac{\partial}{\partial x_j} \right) . V_k \mathbf{e}_k = \mathbf{e}_j . \mathbf{e}_k \frac{\partial V_k}{\partial x_j} = \delta_{jk} \frac{\partial V_k}{\partial x_j}, \tag{1.10}$$

$$\frac{\partial V_j}{\partial x_j} = \mathbf{e}_1 \frac{\partial V_1}{\partial x_1} + \mathbf{e}_2 \frac{\partial V_2}{\partial x_2} + \mathbf{e}_3 \frac{\partial V_3}{\partial x_3}.$$

1.12 Curl of a Vector

The curl of a vector is

$$\nabla \times \mathbf{V} = \left(\mathbf{e}_j \frac{\partial}{\partial x_j} \right) \times V_k \mathbf{e}_k = \mathbf{e}_j \times \mathbf{e}_k \frac{\partial V_k}{\partial x_j}, \tag{1.11}$$

$$\nabla \times \mathbf{V} = \mathbf{e}_1 \left(\frac{\partial V_3}{\partial x_2} - \frac{\partial V_2}{\partial x_3} \right) + \mathbf{e}_2 \left(\frac{\partial V_1}{\partial x_3} - \frac{\partial V_3}{\partial x_1} \right) + \mathbf{e}_3 \left(\frac{\partial V_2}{\partial x_1} - \frac{\partial V_1}{\partial x_2} \right). \tag{1.12}$$

1.13 Divergence of a Tensor

The divergence of a tensor is defined by

$$\nabla . \mathbf{S} = \left(\mathbf{e}_k \frac{\partial}{\partial x_k} \right) . (S_{ij} \mathbf{e}_i \mathbf{e}_j) = \mathbf{e}_j \frac{\partial S_{ij}}{\partial x_i}. \tag{1.13}$$

1.14 Classification of the Fluid Flows

The following terms describe the states which are used to classify fluid flow

1.14.1 Uniform Flow

A flow in which the velocities of the liquid particles at all sections of pipe or channels are equal.

1.14.2 Steady Flow

A flow in which the quantity of fluid flowing per second is constant, that is the velocity, pressure may change from point to point but do not change with time. The steady flow may be uniform or non-uniform.

1.14.3 Laminar Flow

A flow in which each fluid particle has a definite path and the paths of individual particles do not cross each other.

1.14.4 Turbulent Flow

A flow in which fluid particles move haphazardly in all directions. It is impossible to trace the motion of individual particles in turbulent flow.

1.14.5 Viscous and Inviscid Flow

An inviscid flow is one in which viscous effects do not significantly influence the flow and are thus neglected. In a viscous flow the effects of viscosity are important and cannot be ignored.

1.14.6 Compressible Flow

A flow in which volume and thus density of the flowing fluid changes during the flow is called compressible flow.

1.14.7 Incompressible Flow

A flow in which volume and thus density of the flowing fluid does not change during the flow is called incompressible flow.

1.15 Reynolds number

It is dimensionless number. Its is usually denoted by Re. It is the ratio of inertial forces to viscous forces and is denoted by the formula

$$\text{Re} = \frac{\rho V L}{\mu} = \frac{V L}{\nu}, \tag{1.14}$$

where V is characteristic velocity and L is the characteristic length.

1.15.1 Streamline

A streamline is everywhere tangent to the velocity vector at a given instant of time.

1.16 Types of Fluids

1.16.1 Ideal Fluid

An ideal fluid is one that is incompressible and has no viscosity. Ideal fluids do not actually exist , but sometimes it is useful to consider what would happen to an ideal fluid in a particular fluid flow problem in order to simplify the problem.

1.16.2 Viscous Fluids

All fluids for which the dynamic viscosity is not zero are termed as viscous fluid. Viscous fluids include Newtonian and non-Newtonian Fluids.

1.16.3 Newtonian Fluids

Fluids which obey Newtons's Law of viscosity are known as Newtonian fluids.

1.16.4 Non-Newtonian Fluids

Fluids in which shear stress are not linearly proportional to deformation rate are known as non-Newtonian fluids that is

$$\tau_{xy} \neq \mu \left(\frac{du}{dy} \right). \tag{1.15}$$

For non-Newtonian fluids

$$\tau_{xy} = k\left(\frac{du}{dy}\right)^n, n \neq 1, \tag{1.16}$$

where k is flow consistency index and n is flow behavior index. This equation reduces to Newton's law of viscosity if $n = 1$ with $k = \mu$. To ensure that τ_{xy} and du/dy have same signs we write the equation as

$$\tau_{xy} = k\left|\frac{du}{dy}\right|^n = \eta\frac{du}{dy}, \tag{1.17}$$

where the term $\eta = k\,|du/dy|^{n-1}$ is referred to the apparent viscosity or affected viscosity. In a non-Newtonian fluid the viscosity changes with the applied shear force. Ketchup, toothpaste, blood and shampoo are common examples of non-Newtonian fluids.

1.17 Governing Equations

The equations used to describe the motion of the fluid are known as governing equations. The following are the basic governing equations to describe a certain flow.

1.17.1 Continuity Equation

The law of conservation of mass says that the mass of a closed system will remain constant, regardless of the processes acting inside the system. The mathematical form of conservation of mass for compressible fluid is

$$\frac{\partial\rho}{\partial t} + (\nabla.\rho\mathbf{V}) = 0. \tag{1.18}$$

For incompressible fluid above equation simplifies to

$$\nabla.\mathbf{V} = 0. \tag{1.19}$$

that is

$$\frac{\partial u}{\partial x} + \frac{\partial v}{\partial y} + \frac{\partial w}{\partial z} = 0. \tag{1.20}$$

1.17.2 Navier-Stokes Equations

The law of conservation of momentum with usual notation is given by

$$\rho\left[\frac{\partial}{\partial t}+\mathbf{V}\cdot\boldsymbol{\nabla}\right]\mathbf{V}=div\mathbf{T}+\rho\mathbf{f}, \tag{1.21}$$

where $\mathbf{T}$ is Cauchy stress tensor, $\mathbf{f}$ is the body force per unit mass and t is the time.

Generally, $\mathbf{T}$ has the form

$$\mathbf{T}=-p\mathbf{I}+\mathbf{S}, \tag{1.22}$$

where $p\mathbf{I}$ is the indeterminate part of the stress and $\mathbf{S}$ is the extra stress tensor.

For a Newtonian fluid

$$\overline{\mathbf{S}}=\mu\overline{\mathbf{A}}_1-\frac{2}{3}\mu\left(\boldsymbol{\nabla}.\mathbf{V}\right)\bar{\mathbf{I}}, \tag{1.23}$$

where $\overline{\mathbf{A}}_1$ is the first Rivlin-Ericksen tensor given by

$$\mathbf{A}_1=\boldsymbol{\nabla}\mathbf{V}+\left(\boldsymbol{\nabla}\mathbf{V}\right)^T. \tag{1.24}$$

Equation (1.21) in component form can be written as

$$\rho\left[\frac{du}{dt}+u\frac{du}{dx}+v\frac{du}{dy}+w\frac{du}{dz}\right]=-\frac{\partial p}{\partial x}+\frac{\partial S_{xx}}{\partial x}+\frac{\partial S_{xy}}{\partial y}+\frac{\partial S_{xz}}{\partial z}+\rho f_x, \tag{1.25}$$

$$\rho\left[\frac{du}{dt}+u\frac{du}{dx}+v\frac{du}{dy}+w\frac{du}{dz}\right]=-\frac{\partial p}{\partial y}+\frac{\partial S_{xy}}{\partial x}+\frac{\partial S_{yy}}{\partial y}+\frac{\partial S_{yz}}{\partial z}+\rho f_y, \tag{1.26}$$

$$\rho\left[\frac{du}{dt}+u\frac{du}{dx}+v\frac{du}{dy}+w\frac{du}{dz}\right]=-\frac{\partial p}{\partial z}+\frac{\partial S_{zx}}{\partial x}+\frac{\partial S_{zy}}{\partial y}+\frac{\partial S_{zz}}{\partial z}+\rho f_z. \tag{1.27}$$

Similarly from Eq. (1.23) the component of S are:

$$
\begin{aligned}
S_{xy} &= S_{yx} = \mu \left(\frac{\partial v}{\partial x} + \frac{\partial u}{\partial y} \right), && (1.28) \\
S_{yz} &= S_{zy} = \mu \left(\frac{\partial w}{\partial y} + \frac{\partial v}{\partial z} \right), && (1.29) \\
S_{zx} &= S_{xz} = \mu \left(\frac{\partial u}{\partial z} + \frac{\partial w}{\partial x} \right); && (1.30) \\
S_{xx} &= \frac{2}{3} \mu \nabla \cdot \mathbf{V} + 2\mu \frac{\partial u}{\partial x}, && (1.31) \\
S_{yy} &= \frac{2}{3} \mu \nabla \cdot \mathbf{V} + 2\mu \frac{\partial v}{\partial y}, && (1.32) \\
S_{zz} &= \frac{2}{3} \mu \nabla \cdot \mathbf{V} + 2\mu \frac{\partial w}{\partial z}. && (1.33)
\end{aligned}
$$

Substituting the above results into Eqs.(1.25) – (1.27), we arrive at

$$
\rho \left[\frac{\partial u}{\partial t} + u \frac{\partial u}{\partial x} + v \frac{\partial u}{\partial y} + w \frac{\partial u}{\partial z} \right] = \begin{matrix} -\frac{\partial p}{\partial x} + \mu \left(\frac{\partial^2 u}{\partial x^2} + \frac{\partial^2 u}{\partial y^2} + \frac{\partial^2 u}{\partial z^2} \right) \\ \rho f_x + \frac{1}{3} \mu \frac{\partial}{\partial x} \left(\nabla . \mathbf{V} \right) \end{matrix}, \qquad (1.34)
$$

$$
\rho \left[\frac{\partial v}{\partial t} + u \frac{\partial v}{\partial x} + v \frac{\partial v}{\partial y} + w \frac{\partial v}{\partial z} \right] = \begin{matrix} -\frac{\partial p}{\partial y} + \mu \left(\frac{\partial^2 v}{\partial x^2} + \frac{\partial^2 v}{\partial y^2} + \frac{\partial^2 v}{\partial z^2} \right) \\ \rho f_y + \frac{1}{3} \mu \frac{\partial}{\partial y} \left(\nabla . \mathbf{V} \right) \end{matrix}, \qquad (1.35)
$$

$$
\rho \left[\frac{\partial w}{\partial t} + u \frac{\partial w}{\partial x} + v \frac{\partial w}{\partial y} + w \frac{\partial w}{\partial z} \right] = \begin{matrix} -\frac{\partial p}{\partial z} + \mu \left(\frac{\partial^2 w}{\partial x^2} + \frac{\partial^2 w}{\partial y^2} + \frac{\partial^2 w}{\partial z^2} \right) \\ \rho f_w + \frac{1}{3} \mu \frac{\partial}{\partial w} \left(\nabla . \mathbf{V} \right) \end{matrix}. \qquad (1.36)
$$

Eqs. (1.34) – (1.36) are valid for any arbitrary three dimensional and tri-directional flow of a Newtonian fluid.

Chapter 2

Slip effects on the peristaltic flow of a non-Newtonian Maxwellian fluid

This chapter presents a review of the work by El-Shehawy et al. [15]. They have studied the effects of slip at the wall of tube on the peristaltic flow of a compressible Maxwell fluid. All the mathematical expressions and graphical results are re-derived. Some discrepancies are found which are as follows. It is noted that in ref. [15] the expression of $V_{20}(r)$ (Eq. (39) of ref. [15]) is incorrect. In fact the factor $(1 - i\alpha t_m)$ should be 1 for correct comparison. Further, the factor $(1 - i\alpha t_m)$ in Eq. (2.62) (Eq. (41) of ref. [15]) and Eq. (2.68) (Eq. (46) of ref. [15]) should be 1.

2.1 Formulation of the problem

Consider an axisymmetric cylindrical tube (pore) having radius R and length L. A travelling is imposed on the wall (boundary) of the tube with the displacement of the form

$$W(z, t) = R + a\cos\left(\frac{2\pi}{\lambda}(z - ct)\right), \tag{2.1}$$

where a is the amplitude, λ is wave length and c is the speed of the wave, respectively. A cylindrical coordinate system (r, ϕ, z) is employed to investigate the flow with z along the axis of the tube. The velocity field for the flow under consideration is given as

$$\mathbf{v} = \left[v_r\left(r, z, t\right), 0, v_z\left(r, z, t\right)\right], \tag{2.2}$$

where v_r and v_z are the radial and axial velocity components.

To describe the viscoelastic properties of the fluid, the constitutive equation to the Maxwell's model is used, which assumes that

$$\left(1 + t_m \frac{\partial}{\partial t}\right) \mathbf{S} = \mu \overline{A}_1 - \frac{2}{3}\mu \left(\mathbf{\nabla}.\mathbf{V}\right) \mathbf{I}, \tag{2.3}$$

where t_m is rèlaxation time.

It is further assumed the following equation of state holds

$$\frac{1}{\rho}\frac{\partial \rho}{\partial p} = k^*, \tag{2.4}$$

where k^* is the compressibility of the liquid. The solution of this equation for the density as a function of the pressure is given by

$$\rho = \rho_0 e^{\left[k^* \left(\rho - \rho_0\right)\right]}, \tag{2.5}$$

where ρ_0 is the constant density at the reference pressure p_0.

The boundary conditions that must be satisfied by the fluid on the wall are the slip conditions. For the slip flow the fluid still obeys the Navier-Stokes equation, but the no-slip condition is replaced by the slip condition $u_t = A_p \partial u / \partial n$, where u_t is the tangential velocity, n is the normal to the surface, and A_p is the coefficient close to mean free path of the molecules of the fluid. This condition has been attributed to Beavers and Joseph for a porous boundary but it was Navier who proposed it a century ago. Although the Navier condition looked simple, analytically it is much more difficult than the no slip condition. Thus the boundary conditions at the wall are

$$v_r\left(W, z, t\right) = \frac{\partial W}{\partial t}, \; v_z\left(W, z, t\right) = A\frac{\partial v_z}{\partial r}, \tag{2.6}$$

where A is the mean free path of the molecules of the liquid.

Utilizing Eqs. (1.23) and (2.3) into Eq. (1.21) and neglecting the body force one can write

$$\left(1+t_m\frac{\partial}{\partial t}\right)\left(\rho\frac{\partial \mathbf{v}}{\partial t}+\rho(\mathbf{v}.\boldsymbol{\nabla})\mathbf{v}\right)=-\left(1+t_m\frac{\partial}{\partial t}\right)\boldsymbol{\nabla}p+\mu\left[\overline{A}_1-\frac{2}{3}\left(\boldsymbol{\nabla}.\mathbf{V}\right)\mathbf{I}\right]. \tag{2.7}$$

In cylindrical coordinates, the mass balance equation (1.18) can be written as

$$\frac{\partial \rho}{\partial t}+v_r\frac{\partial \rho}{\partial r}+v_z\frac{\partial \rho}{\partial z}+\rho\left(\frac{\partial v_r}{\partial r}+\frac{v_r}{r}+\frac{\partial v_z}{\partial z}\right)=0, \tag{2.8}$$

while Eq. (2.7) in scalar form become

$$\begin{aligned}\left(1+t_m\frac{\partial}{\partial t}\right)\left[\rho\frac{\partial v_r}{\partial t}+\rho\left(v_r\frac{\partial v_r}{\partial r}+v_z\frac{\partial v_r}{\partial z}\right)\right]= &-\left(1+t_m\tfrac{\partial}{\partial t}\right)\tfrac{\partial p}{\partial r}+\mu\left(\tfrac{\partial^2 v_r}{\partial r^2}+\tfrac{1}{r}\tfrac{\partial v_r}{\partial r}-\tfrac{v_r}{r^2}+\tfrac{\partial^2 v_r}{\partial z^2}\right)\\ &+\tfrac{\mu}{3}\tfrac{\partial}{\partial r}\left(\tfrac{\partial v_r}{\partial r}+\tfrac{v_r}{r}+\tfrac{\partial v_z}{\partial z}\right),\end{aligned} \tag{2.9}$$

$$\begin{aligned}\left(1+t_m\frac{\partial}{\partial t}\right)\left[\rho\frac{\partial v_z}{\partial t}+\rho\left(v_r\frac{\partial v_z}{\partial r}+v_z\frac{\partial v_z}{\partial z}\right)\right]= &-\left(1+t_m\tfrac{\partial}{\partial t}\right)\tfrac{\partial p}{\partial z}+\mu\left(\tfrac{\partial^2 v_z}{\partial r^2}+\tfrac{1}{r}\tfrac{\partial v_z}{\partial r}+\tfrac{\partial^2 v_z}{\partial z^2}\right)\\ &+\tfrac{\mu}{3}\tfrac{\partial}{\partial z}\left(\tfrac{\partial v_r}{\partial r}+\tfrac{v_r}{r}+\tfrac{\partial v_z}{\partial z}\right).\end{aligned} \tag{2.10}$$

It would be expedient to simplify these equations by introducing non-dimensional variables. There is a characteristic velocity c and characteristic lengths a, λ and R. The following variables based on c and R could thus be introduced:

$$\overline{W}=\frac{W}{R},\ \overline{v_r}=\frac{v_r}{c},\ \overline{v_z}=\frac{v_z}{c},\ \overline{\rho}=\frac{\rho}{\rho_0},\ \overline{p}=\frac{p}{\rho_0c^2},\ \overline{p_0}=\frac{p_0}{\rho_0c^2},\ \overline{t}=\frac{ct}{R}. \tag{2.11}$$

The amplitude ratio ϵ, the wave number α, the Reynolds number Re, the Knudsen number Kn and the compressibility number χ are defined by

$$\epsilon=\frac{a}{R},\ \alpha=\frac{2\pi R}{\lambda},\ \mathrm{Re}=\frac{\rho_0cR}{\mu},\ Kn=\frac{A}{R},\ \chi=k^*\rho_0c^2. \tag{2.12}$$

Under the above assumptions Eqs. (2.5) and(2.8) – (2.10) can be rewritten in the non-dimensional form after dropping the bar as

$$\frac{\partial \rho}{\partial t}+v_r\frac{\partial \rho}{\partial r}+v_z\frac{\partial \rho}{\partial z}+\rho\left(\frac{\partial v_r}{\partial r}+\frac{v_r}{r}+\frac{\partial v_z}{\partial z}\right)=0, \tag{2.13}$$

$$\left(1+t_m\frac{\partial}{\partial t}\right)\left[\rho\frac{\partial v_r}{\partial t}+\rho\left(v_r\frac{\partial v_r}{\partial r}+v_z\frac{\partial v_r}{\partial z}\right)\right]= \begin{array}{l} -\left(1+t_m\frac{\partial}{\partial t}\right)\frac{\partial p}{\partial r}+\frac{1}{\mathrm{Re}}\left(\frac{\partial^2 v_r}{\partial r^2}+\frac{1}{r}\frac{\partial v_r}{\partial r}-\frac{v_r}{r^2}+\frac{\partial^2 v_r}{\partial z^2}\right) \\ +\frac{1}{3\,\mathrm{Re}}\frac{\partial}{\partial r}\left(\frac{\partial v_r}{\partial r}+\frac{v_r}{r}+\frac{\partial v_z}{\partial z}\right), \end{array} \tag{2.14}$$

$$\left(1+t_m\frac{\partial}{\partial t}\right)\left[\rho\frac{\partial v_z}{\partial t}+\rho\left(v_r\frac{\partial v_z}{\partial r}+v_z\frac{\partial v_z}{\partial z}\right)\right]= \begin{array}{l} -\left(1+t_m\frac{\partial}{\partial t}\right)\frac{\partial p}{\partial z}+\frac{1}{\mathrm{Re}}\left(\frac{\partial^2 v_z}{\partial r^2}+\frac{1}{r}\frac{\partial v_z}{\partial r}+\frac{\partial^2 v_z}{\partial z^2}\right) \\ +\frac{1}{3\,\mathrm{Re}}\frac{\partial}{\partial z}\left(\frac{\partial v_r}{\partial r}+\frac{v_r}{r}+\frac{\partial v_z}{\partial z}\right), \end{array} \tag{2.15}$$

$$\rho=e^{\chi(\rho-\rho_0)}. \tag{2.16}$$

also the boundary conditions (2.6) becomes

$$v_r\left((1+\eta),z,t\right)=\frac{\partial\eta\left(z,t\right)}{\partial t},\quad v_z\left((1+\eta),z,t\right)=Kn\frac{\partial v_z\left(r,z,t\right)}{\partial r}, \tag{2.17}$$

where

$$\eta\left(z,t\right)=\epsilon\cos\alpha\left(z-t\right). \tag{2.18}$$

2.2 Method of solution

Assuming the solution of the governing equations in a form [11]

$$\begin{aligned} p &= p_0+\epsilon p_1(r,z,t)+\epsilon^2 p_2(r,z,t)+\ldots.., \\ v_r &= \epsilon u_1(r,z,t)+\epsilon^2 u_2(r,z,t)+\ldots.., \\ v_z &= \epsilon v_1(r,z,t)+\epsilon^2 v_2(r,z,t)+\ldots.., \\ \rho &= 1+\epsilon\rho_1(r,z,t)+\epsilon^2\rho_2(r,z,t)+\ldots.. \end{aligned} \tag{2.19}$$

and doing a usual perturbation analysis one can obtain a closed set of governing equations for the first (ϵ) and second (ϵ^2) order as the following:

$$\left(1+t_m\frac{\partial}{\partial t}\right)\frac{\partial u_1}{\partial t}=\begin{array}{l}-\left(1+t_m\frac{\partial}{\partial t}\right)\frac{\partial p_1}{\partial r}+\frac{1}{\mathrm{Re}}\left(\frac{\partial^2 u_1}{\partial r^2}+\frac{1}{r}\frac{\partial u_1}{\partial r}-\frac{u_1}{r^2}+\frac{\partial^2 u_1}{\partial z^2}\right)\\ +\frac{1}{3\,\mathrm{Re}}\frac{\partial}{\partial r}\left(\frac{\partial u_1}{\partial r}+\frac{u_1}{r}+\frac{\partial v_1}{\partial z}\right),\end{array} \tag{2.20}$$

$$\left(1+t_m\frac{\partial}{\partial t}\right)\frac{\partial v_1}{\partial t}=\begin{array}{l}-\left(1+t_m\frac{\partial}{\partial t}\right)\frac{\partial p_1}{\partial z}+\frac{1}{\mathrm{Re}}\left(\frac{\partial^2 v_1}{\partial r^2}+\frac{1}{r}\frac{\partial v_1}{\partial r}+\frac{\partial^2 v_1}{\partial z^2}\right)\\ +\frac{1}{3\,\mathrm{Re}}\frac{\partial}{\partial z}\left(\frac{\partial u_1}{\partial r}+\frac{u_1}{r}+\frac{\partial v_1}{\partial z}\right),\end{array} \tag{2.21}$$

$$\frac{\partial \rho_1}{\partial t}+\frac{\partial u_1}{\partial r}+\frac{u_1}{r}+\frac{\partial v_1}{\partial z}=0, \tag{2.22}$$

$$\rho_1=\chi p_1, \tag{2.23}$$

$$\left(1+t_m\frac{\partial}{\partial t}\right)\left(\frac{\partial u_2}{\partial t}+\rho_1\frac{\partial u_1}{\partial t}+u_1\frac{\partial u_1}{\partial r}+v_1\frac{\partial u_1}{\partial z}\right)=\begin{array}{l}-\left(1+t_m\frac{\partial}{\partial t}\right)\frac{\partial p_2}{\partial r}+\frac{1}{\mathrm{Re}}\left(\frac{\partial^2 u_2}{\partial r^2}+\frac{1}{r}\frac{\partial u_2}{\partial r}-\frac{u_2}{r^2}+\frac{\partial^2 u_2}{\partial z^2}\right)\\ +\frac{1}{3\,\mathrm{Re}}\frac{\partial}{\partial r}\left(\frac{\partial u_2}{\partial r}+\frac{u_2}{r}+\frac{\partial v_2}{\partial z}\right),\end{array} \tag{2.24}$$

$$\left(1+t_m\frac{\partial}{\partial t}\right)\left(\frac{\partial v_2}{\partial t}+\rho_1\frac{\partial v_1}{\partial t}+u_1\frac{\partial v_1}{\partial r}+v_1\frac{\partial v_1}{\partial z}\right)=\begin{array}{l}-\left(1+t_m\frac{\partial}{\partial t}\right)\frac{\partial p_2}{\partial z}+\frac{1}{\mathrm{Re}}\left(\frac{\partial^2 v_2}{\partial r^2}+\frac{1}{r}\frac{\partial v_2}{\partial r}+\frac{\partial^2 v_2}{\partial z^2}\right)\\ +\frac{1}{3\,\mathrm{Re}}\frac{\partial}{\partial z}\left(\frac{\partial u_2}{\partial r}+\frac{u_2}{r}+\frac{\partial v_2}{\partial z}\right),\end{array} \tag{2.25}$$

$$\frac{\partial \rho_2}{\partial t}+u_1\frac{\partial \rho_1}{\partial r}+v_1\frac{\partial \rho_1}{\partial z}+\frac{u_2}{r}+\frac{\partial u_2}{\partial r}+\frac{\partial v_2}{\partial z}+\rho_1\left(\frac{\partial u_1}{\partial r}+\frac{u_1}{r}+\frac{\partial v_1}{\partial z}\right)=0, \tag{2.26}$$

$$\rho_2=\chi p_2+\frac{1}{2}\chi^2 p_1^2. \tag{2.27}$$

Expanding Eq. (2.17) by Taylor expansion around $r=1$ and substituting from Eq. (2.19) one gets the following boundary conditions:

$$u_1\left(1,z,t\right)=-\frac{i\alpha}{2}(e^{i\alpha(z-t)}-e^{-i\alpha(z-t)}), \tag{2.28}$$

$$u_2(1,z,t) + \frac{1}{2}\left(e^{i\alpha(z-t)} - e^{-i\alpha(z-t)}\right)\frac{\partial u_1}{\partial r}(1,z,t) = 0, \tag{2.29}$$

$$v_1(1,z,t) = Kn\frac{\partial v_1}{\partial r}(1,z,t), \tag{2.30}$$

$$\begin{aligned} &v_2(1,z,t) + \tfrac{1}{2}\left(e^{i\alpha(z-t)} - e^{-i\alpha(z-t)}\right)\tfrac{\partial v_1}{\partial r}(1,z,t) = \\ &Kn\left[\tfrac{\partial v_2}{\partial r}(1,z,t) + \tfrac{1}{2}\left(e^{i\alpha(z-t)} - e^{-i\alpha(z-t)}\right)\tfrac{\partial^2 v_1}{\partial r^2}(1,z,t)\right]. \end{aligned} \tag{2.31}$$

Following [11] the solution of the linear problem can be assumed in the form

$$\begin{aligned} u_1(r,z,t) &= U_1(r)e^{i\alpha(z-t)} + \overline{U}_1 e^{-i\alpha(z-t)}, \\ v_1(r,z,t) &= V_1(r)e^{i\alpha(z-t)} + \overline{V}_1 e^{-i\alpha(z-t)}, \\ p_1(r,z,t) &= P_1(r)e^{i\alpha(z-t)} + \overline{P}_1 e^{-i\alpha(z-t)}, \\ \rho_1(r,z,t) &= \chi P_1(r)e^{i\alpha(z-t)} + \chi\overline{P}_1 e^{-i\alpha(z-t)}. \end{aligned} \tag{2.32}$$

Here and in the following equations, the bar denotes a complex conjugate.

On the other hand the second (ϵ^2) order solution can be written as

$$\begin{aligned} u_2(r,z,t) &= U_{20}(r) + U_2(r)e^{2i\alpha(z-t)} + \overline{U}_2 e^{-2i\alpha(z-t)}, \\ v_2(r,z,t) &= V_{20}(r) + V_2(r)e^{2i\alpha(z-t)} + \overline{V}_2 e^{-2i\alpha(z-t)}, \\ p_2(r,z,t) &= P_{20}(r) + P_2(r)e^{2i\alpha(z-t)} + \overline{P}_2 e^{-2i\alpha(z-t)}, \\ \rho_2(r,z,t) &= D_{20}(r) + D_2(r)e^{2i\alpha(z-t)} + \overline{D}_2 e^{-2i\alpha(z-t)}. \end{aligned} \tag{2.33}$$

The latter choice of solution is motivated by the fact that the peristaltic flow is essentially a nonlinear (second order) effect and adding non oscillatory term in the first order gives only a trivial solution. Thus, one can add non oscillatory terms, such as $U_{20}(r), V_{20}(r), P_{20}(r)$ and $D_{20}(r)$, which do not cancel out in the solution after time averaging over the period, only in the second order and higher orders.

Substituting from Eq. (2.32) into Eqs. (2.20) – (2.23) and (2.28) – (2.31) the following system of equations are obtained.

$$-i\alpha\left(1-i\alpha t_m\right)U_1 = \begin{array}{c} -\left(1-i\alpha t_m\right)P_1' + \frac{1}{\mathrm{Re}}\left(U_1'' + \frac{U_1'}{r} - \frac{U_1}{r^2} - \alpha^2 U_1\right) \\ +\frac{1}{3\,\mathrm{Re}}\frac{d}{dr}\left(U_1' + \frac{U_1}{r} + i\alpha V_1\right), \end{array} \tag{2.34}$$

$$-i\alpha\left(1-i\alpha t_m\right)V_1 = \begin{array}{c} -i\alpha(1-i\alpha t_m)P_1 + \frac{1}{\mathrm{Re}}\left(V_1'' + \frac{V_1'}{r} - \alpha^2 V_1\right) \\ +\frac{i\alpha}{3\,\mathrm{Re}}\left(U_1' + \frac{U_1}{r} + i\alpha V_1\right), \end{array} \tag{2.35}$$

$$U_1' + \frac{U_1}{r} + i\alpha V_1 = i\alpha\chi P_1. \tag{2.36}$$

$$U_1(1) = \frac{-i\alpha}{2}. \tag{2.37}$$

$$V_1(1) = KnV_1'(1). \tag{2.38}$$

Here the prime denotes a derivative with respect to r.

A rearrangement of the system of Eqs. (2.34) – (2.36) yields

$$-\gamma P_1' + \left(U_1'' + \frac{U_1'}{r} - \frac{U_1}{r^2} - \beta^2 U_1\right) = 0. \tag{2.39}$$

$$-\gamma P_1 - \frac{i}{\alpha}\left(V_1'' + \frac{V_1'}{r} - \beta^2 V_1\right) = 0. \tag{2.40}$$

where the complex parameters γ and β are given by

$$\gamma = (1-i\alpha t_m)\,\mathrm{Re} - \frac{i\alpha\chi}{3}, \ \beta^2 = \alpha^2 - i\alpha(1-i\alpha t_m)\,\mathrm{Re}. \tag{2.41}$$

Eliminating $V_1(r)$ by using Eq. (2.36), one can rewrite Eq. (2.40) as

$$-\frac{i\chi}{\alpha}\left[P_1'' + \frac{P_1'}{r} - \left(\beta^2 + \frac{i\alpha\gamma}{\chi}\right)P_1\right] + \frac{1}{\alpha^2}\left(\frac{d}{dr} + \frac{1}{r}\right)\left[U_1'' + \frac{U_1'}{r} - \frac{U_1}{r^2} - \beta^2 U_1\right] = 0. \tag{2.42}$$

Differentiating Eq. (2.42) with respect to r and using Eq. (2.39) give the following equation:

$$\begin{aligned} -\left[\frac{i\chi}{\alpha\gamma}\frac{d^2}{dr^2}+\frac{1}{r}\frac{d}{dr}-\frac{1}{r^2}-\left(\beta^2+\frac{i\alpha\gamma}{\chi}\right)\right]\left(U_1'+\frac{U_1'}{r}-\frac{U_1}{r^2}-\beta^2 U_1\right) \\ +\frac{1}{\alpha^2}\left(\frac{d^2}{dr^2}+\frac{d}{dr}-\frac{1}{r^2}\right)\left(U_1'+\frac{U_1'}{r}-\frac{U_1}{r^2}-\beta^2 U_1\right)=0. \end{aligned} \tag{2.43}$$

This equation is rewritten, after multiplication by α^2 as

$$\left(1-\frac{i\chi\alpha}{\gamma}\right)\left(\frac{d^2}{dr^2}+\frac{1}{r}\frac{d}{dr}-\frac{1}{r^2}-\nu^2\right)\left(\frac{d^2}{dr^2}+\frac{d}{dr}-\frac{1}{r^2}-\beta^2\right)U_1=0, \tag{2.44}$$

where

$$\nu^2=\alpha^2\frac{(1-\chi)\,(1-i\alpha t_m)\,\mathrm{Re}-(4/3)\,i\alpha\chi}{(1-i\alpha t_m)\,\mathrm{Re}-(4/3)\,i\alpha\chi}. \tag{2.45}$$

From this equation (2.44) one obtains master equation for $U_1(r)$ and find its general solution as

$$U_1(r)=C_1 I_1(\nu r)+C_2 I_1(\beta r), \tag{2.46}$$

where I_1 is the modified Bessel function of the first kind of order one. Note, that Eq. (2.46) is similar to Eq. (3.18) in [11], except that C_1 and C_2 are complex constants calculated using Eqs. (2.37) – (2.38) and defined by

$$C_1=\frac{i\alpha\beta\nu\left[I_0(\beta)-\beta Kn I_1(\beta)\right]}{2\left[\alpha^2 I_1(\beta)I_0(\nu)-\beta\nu I_0(\beta)I_1(\nu)+\nu Kn I_1(\beta)I_1(\nu)\left(\beta^2-\alpha^2\right)\right]}, \tag{2.47}$$

$$C_2=\frac{-i\alpha^3\left[I_0(\nu)-\nu Kn I_1(\nu)\right]}{2\left[\alpha^2 I_1(\beta)I_0(\nu)-\beta\nu I_0(\beta)I_1(\nu)+\nu Kn I_1(\beta)I_1(\nu)\left(\beta^2-\alpha^2\right)\right]}. \tag{2.48}$$

Here I_0 is the modified Bessel function of the first kind of order zero

The general solution for $V_1(r)$ is

$$V_1(r)=\frac{i\alpha C_1}{\nu}I_0(\nu r)+\frac{i\beta C_2}{\alpha}I_0(\beta r), \tag{2.49}$$

and the general solution for $P_1(r)$:

$$P_1(r) = \frac{C_1(\nu^2 - \beta^2)}{\gamma\nu} I_0(\nu r). \tag{2.50}$$

Employing the same procedure as for the solution of system of order ϵ one obtains the following set of equations

$$D_{20} = \chi P_{20} + \chi^2 P_1 \overline{P_1}, \tag{2.51}$$

$$U_{20}' + \frac{U_{20}}{r} = -\chi\left(P_1\overline{U_1'} + \overline{P_1}U_1' + \frac{P_1\overline{U_1}}{r} + \frac{\overline{P_1}U_1}{r} + \overline{P_1'}U_1 + P_1'\overline{U_1}\right), \tag{2.52}$$

$$i\alpha\chi P_1\overline{U_1} - i\alpha\chi\overline{P_1}U_1 + U_1\overline{U_1'} + U_1'\overline{U_1} + i\alpha\overline{V_1}U_1 - i\alpha V_1\overline{U_1} = \begin{array}{l} -P_{20}' + \frac{1}{\mathrm{Re}}\left(U_{20}' + \frac{U_{20}'}{r} - \frac{U_{20}}{r^2}\right) \\ +\frac{1}{3\,\mathrm{Re}}\frac{d}{dr}\left(U_{20}' + \frac{U_{20}}{r}\right), \end{array} \tag{2.53}$$

$$i\alpha\chi P_1\overline{V_1} - i\alpha\chi\overline{P_1}V_1 + U_1\overline{V_1'} + \overline{U_1}V_1' = \frac{1}{\mathrm{Re}}\left(V_{20}' + \frac{V_{20}'}{r}\right), \tag{2.54}$$

$$U_{20}(1) + \frac{1}{2}\left(\overline{U_1'}(1) + U_1'(1)\right) = 0, \tag{2.55}$$

$$V_{20}(1) + \frac{1}{2}\left(\overline{V_1'}(1) + V_1'(1)\right) = Kn\left(V_{20}'(1) + \frac{1}{2}V_1'(1) + \frac{1}{2}\overline{V_1'}(1)\right). \tag{2.56}$$

It will be seen that, as far as the net flow is considered, only the functions U_{20}, V_{20}, P_{20} and D_{20} contribute to the net flow as long as terms up to $O(\epsilon^2)$ are retained. Thus, the functions U_2, V_2, P_2 and D_2 do not contribute to the net flow, and therefore the equations satisfied by them will not written nor their solution will performed. In the next the solutions for U_{20}, V_{20}, P_{20} and D_{20} will be computed.The second-order solution $U_{20}(r)$ can also be found in a way similar to the one used in the first order as follows:

$$U_{20}(r) = \frac{D_1}{r} - \chi\left[P_1(r)\overline{U_1}(r) + \overline{P_1}(r)U_1(r)\right], \tag{2.57}$$

where D_1 is a complex constant (which follows from the boundary conditions (2.55)) defined by

$$D_1 = \frac{i\alpha Kn}{2}\left(V_1'(1) - \overline{V_1'}(1)\right), \tag{2.58}$$

having the final form

$$D_1 = \frac{i\alpha Kn}{2}\left(i\alpha C_1 I_1(\nu) + \frac{i\beta^2 C_2}{\alpha} I_1(\beta) + i\alpha \overline{C_1} I_1(\overline{\nu}) + \frac{i\overline{\beta}^2\overline{C_2}}{\alpha} I_1(\overline{\beta})\right). \tag{2.59}$$

The general solution for $V_{20}(r)$ is as follows:

$$V_{20}(r) = D_2 - \mathrm{Re}\int_r^1 \left[V_1(\tau)\overline{U_1}(\tau) + \overline{V_1}(\tau)U_1(\tau)\right] d\tau, \tag{2.60}$$

where D_2 is a complex constant defined by

$$D_2 = -\frac{1}{2}\left(\overline{V_1'}(1) + V_1'(1)\right) + Kn\left(V_{20}'(1) + \frac{1}{2}V_1''(1) + \frac{1}{2}\overline{V_1''}(1)\right), \tag{2.61}$$

where the values of $V_{20}'(1)$ and $V_1''(1)$ are defined by

$$V_{20}'(1) = \mathrm{Re}\left[\begin{array}{l} \frac{i\alpha C_1\overline{C_1}}{\upsilon} I_0(\nu)I_1(\overline{\nu}) + \frac{i\alpha C_1\overline{C_2}}{\upsilon} I_0(\nu)I_1(\overline{\beta}) + \frac{i\beta C_2\overline{C_1}}{\alpha} I_0(\beta)I_1(\overline{\nu}) \\ + \frac{i\beta C_2\overline{C_2}}{\alpha} I_0(\beta)I_1(\overline{\beta}) - \frac{i\alpha C_1\overline{C_1}}{\overline{\upsilon}} I_0(\overline{\nu})I_1(\nu) - \frac{i\alpha C_2\overline{C_1}}{\overline{\upsilon}} I_0(\overline{\nu})I_1(\beta) \\ - \frac{i\overline{\beta} C_1\overline{C_2}}{\alpha} I_0(\overline{\beta})I_1(\nu) - \frac{i\overline{\beta} C_2\overline{C_2}}{\alpha} I_0(\overline{\beta})I_1(\beta) \end{array}\right], \tag{2.62}$$

$$V_1''(1) = i\alpha C_1\left(\nu I_0(\nu) - I_1(\nu)\right) + \frac{i\beta^2 C_2}{\alpha}\left(\beta I_0(\beta) - I_1(\beta)\right). \tag{2.63}$$

The dimensionless fluid flow rate Q can be calculated as

$$Q(z,t) = 2\pi\left[\epsilon\int_0^1 v_1(r,z,t)rdr + \epsilon^2\int_0^1 v_2(r,z,t)rdr + O(\epsilon^2)\right]. \tag{2.64}$$

Next, the net flow is considered over one period of time. The average of a variable G over one period T of time t is

$$\langle G\rangle = \frac{1}{T}\int_0^T G(r,z,t)dt. \tag{2.65}$$

At $T = 2\pi/\alpha$, consequently the mean net axial velocity $\langle V_z \rangle$ read

$$\langle V_z \rangle = \epsilon^2 V_{20}(r), \tag{2.66}$$

under neglect of $O(\epsilon^2)$-terms, while the net flow rate $\langle Q \rangle$ is given by

$$\langle Q \rangle = 2\pi\epsilon^2 \int_0^1 v_{20}\,(r)\, r dr. \tag{2.67}$$

under neglect of $O(\epsilon^2)$-terms. Thus, the travelling wave induces a net flow of the liquid, of which the (dimensionless) rate is expressed by Eq. (2.67). Hence, the net flow and the mean net axial velocity are an effect of order ϵ^2.

2.3 Numerical results and discussion

To study the behavior of net flow rate, numerical calculations for several values of α, Kn, t_m and χ are carried out. It is clear that one has to choose $\epsilon << 1$ because of the use of perturbation method with the amplitude ratio ϵ as a perturbation parameter [22]. Also for the perturbation method to be valid and accurate $\epsilon\alpha^2 \,\mathrm{Re} << 1$ according to Takabatake [21].

Now consider the net flow rate $\langle Q \rangle$ given by equation (2.67). After one integration by parts, $\langle Q \rangle$ can be expressed as

$$\langle Q \rangle = \pi\epsilon^2 \left(D_2 - \mathrm{Re} \int_0^1 \left[V_1(r)\overline{U_1}(r) + \overline{V_1}(r) U_1(r) \right] dr \right), \tag{2.68}$$

where the solution of Eq. (2.60) for $V_{20}(r)$ is used.

A numerical code has been written to calculate $\langle Q \rangle$ according to Eq. (2.68). In order to check the validity of the code, it has been run for the parameters similar to the ones used by other authors. For instance, for $\epsilon = 0.15$, $\mathrm{Re} = 100$, $\alpha = 0.2$, $\chi = 0.0$, $t_m = 0.0$ and $Kn = 0.0$ it gives $\langle Q \rangle = 0.2709$, which is equal (which is equal if we keep four digits after the decimal point) to the result of authors [18], who actually obtained $\langle Q \rangle = 0.2709$. This corroborate the validity of the present code. It should be noted that Eq. (2.68) will be identical to the similar equation (4.1) of [11] if one set $Kn = 0.0$ and $t_m = 0$ in all present equations. Further, Eq.(2.68) will be identical to the similar equation (16) of [14] if one set $Kn = 0.0$ in all presented equations.

Firstly, the effect of slip boundary conditions in the case of a Newtonian ($t_m = 0$) fluid are investigated. The result of calculations are presented in Fig. 1, where the dependence of $\langle Q\rangle$ on the compressibility factor χ for various values of Kn is investigated. It is noticed that the range of $\langle Q\rangle$ is approximately $0.4272 - 2.7043$ for the range of χ from 0 to 1. In particular, for $\chi = 0.0$ the range of $\langle Q\rangle$ is just $1.2305 - 1.4714 \times 10^{-5}$ for the three considered values of Kn, while for $\chi > 0$ the range becomes $0.0034 - 3.8223 \times 10^{-5}$. Hence, $\langle Q\rangle$ is weakly affected by Kn at $\chi = 0.0$. For $\chi > 0$, $\langle Q\rangle$ strongly depends on the Knudsen number of slip flow. Furthermore, we observe that for $Kn = 0.0$, $\langle Q\rangle$ attains a maximum of 2.7141×10^{-5} at $\chi = 0.5$, and for $\chi > 0.5$ the flow decreases to 0.4901×10^{-5}, while for $Kn = 0.05$ $\langle Q\rangle$ attains a maximum of 2.9734×10^{-5} at $\chi = 0.4$, and for $\chi > 0.4$ the flow rate decreases until it reaches 0.2075×10^{-5}, for $Kn = 0.1$ $\langle Q\rangle$ attains a maximum of 3.8226×10^{-5} at $\chi = 0.3$, and for $\chi > 0.3$ the flow rate decreases until it reaches 0.0035×10^{-5}. Thus, it is considered that at high values of Kn the rate of decreasing of $\langle Q\rangle$ is greater than at low values. Furthermore, the compressibility factor χ has a significant influence on the net flow rate, and the Knudsen number Kn plays a more significant role in the net flow of a compressible liquid than of an incompressible one.

Fig. 2 investigates the behavior of the net flow rate $\langle Q\rangle$ depending on the parameter α, which is the tube radius measured in wavelengths. It is seen that the net flow rate $\langle Q\rangle$ attains a maximum for a certain value of α, and this maximum increases with increasing Kn. Furthermore, after $\langle Q\rangle$ reaches the maximum value it then decreases with increasing α, but this decrease is greatest at high values of Kn. Also it is noted that $\langle Q\rangle$ is nearly independent of Kn for $\alpha < 0.001$.

Secondly, the effect of slip boundary conditions in the case of non-Newtonian Maxwellian fluid are investigated. It is known that viscoelastic fluids, described by the Maxwellian fluid, have different flow regimes depending on the value of the parameter $D_e = t_v/t_m$, which is called the Deborah number. In effect, the Deborah number is a ratio of the characteristic time of viscous effects $t_v = \rho R^2/\mu$ to the relaxation time t_m. As noted in, the value of the parameter D_e (which the authors of [19] actually call α) determines in which regime the system resides. Beyond a certain critical value ($D_e = 11.64$), the system is dissipative and conventional viscous effects dominate. On the other hand, for small $D_e (D_e < D_{e_c})$ the system exhibits viscoelastic behavior.

Figure 3 present the dependence of $\langle Q\rangle$ on the compressibility parameter χ for various values of Kn.

When $Kn = 0.0$ it is assumed that the net flow rate reaches a maximum value $\langle Q\rangle = 2.4918\times 10^{-5}$ at $\chi = 0.8$. Further, when $Kn = 0.05$ it is noted that maximum value $\langle Q\rangle = 2.6858\times 10^{-5}$ at $\chi = 0.7$. The maximum value of $\langle Q\rangle = 3.2682\times 10^{-5}$ and occurs at $\chi = 0.6$ when $Kn = 0.1$. From the above discussion, we notice that $\langle Q\rangle$ attains a maximum for a certain value of χ and this maximum increases with increasing Kn. Moreover, there is shifting the maximum value of $\langle Q\rangle$ towards lower values of $\chi's$ with increasing Kn.

Fig. 4 illustrates the behavior of the flow rate $\langle Q\rangle$ depending on the compressibility parameter χ at $t_m = 10000$ (deeply non-Newtonian regime).

In this deeply non-Newtonian regime it is seen that when $Kn = 0.0$ the maximum value of $\langle Q\rangle = 7.2545\times 10^{-5}$ at $\chi = 1.0$, whereas when $Kn = 0.03$ the maximum value of $\langle Q\rangle = 11.3979\times 10^{-5}$ at $\chi = 0.95$ and when $Kn = 0.05$ the maximum value of $\langle Q\rangle = 15.4801\times 10^{-5}$ at $\chi = 0.9$. Thus, in the absence of slip $\langle Q\rangle$ increases with increasing χ in the deeply non-Newtonian regime. On the other hand, when the slip effect is taken into account, it is observed that $\langle Q\rangle$ attains a maximum at a certain value of χ and then decreases. Moreover, there is a shift in the maximum value of $\langle Q\rangle$ towards lower value of χ with increasing Kn.

A comparison of Figs. 1, 3 and 4 shows that when $Kn = 0.05$, the maximum value of $\langle Q\rangle$ is 2.9734×10^{-5} at $t_m = 0.0$ and $\chi = 0.4$, while the maximum value of $\langle Q\rangle$ is 2.6858×10^{-5} at $\chi = 0.7$ and $t_m = 1000$. Moreover, the maximum value of $\langle Q\rangle$ is 15.4801×10^{-5} at $\chi = 0.9$ and $t_m = 10000$. It can be noted from the previous values that the slip boundary condition is affected stronger in the case of a non-Newtonian regime than a Newtonian one. Furthermore, the slip boundary conditions are weakly affected at compressible liquid ($\chi > 0.0$).

In Fig. 5 the dimensionless net flow rate $\langle Q\rangle$ is plotted versus α, which is the tube radius measured in wavelengths, for the following set of parameters: $\epsilon = 0.001$, $\mathrm{Re} = 10000.0$, $\chi = 0.6$ and $t_m = 100$. Note that for $\alpha < 0.001$ the range of net flow rate $\langle Q\rangle$ is $0.0367 - .0791\times 10^{-4}$ at various values of $Kn(0.0 \le Kn \le 0.1)$. Hence, the net flow rate $\langle Q\rangle$ is nearly independent of Kn for $\alpha < 0.001$. For $0.001 \le \alpha \le 0.0065$ it attains a maximum for a certain value of α and this maximum increase with increasing Kn. For $\alpha > 0.0065$ we observe that $\langle Q\rangle$ decreases with increasing Kn. Further at $Kn = 0.0$ there is no negative value of $\langle Q\rangle$. Moreover $\langle Q\rangle =$

-0.0113×10^{-4} reaches negative value at $Kn = 0.05$ and $\alpha = 0.009$, while $\langle Q \rangle = -0.0196 \times 10^{-4}$ at $Kn = 0.075$ and $\alpha = 0.008$, and $\langle Q \rangle = -0.0074 \times 10^{-4}$ at $Kn = 0.1$ and $\alpha = 0.007$. The negative value of net flow rate $\langle Q \rangle$ means the occurrence of back flow. This means flow occurs in the direction opposite to the direction of propagation of the travelling wave on the tube wall. Moreover, the reverse flow (back flow) occurs easily in the presence of slip boundary condition and also a non-Newtonian regime. The net flow rate $\langle Q \rangle$ increases in the reverse direction with increasing α.

In the Fig. 6 the dimensionless net flow rate $\langle Q \rangle$ is plotted versus α for the following set of parameters: $\epsilon = 0.001$, Re $= 10000.0$, $\chi = 0.6$ and $t_m = 1000$. Observed that there is no back flow at $Kn = 0.0$, while $\langle Q \rangle = -0.0019 \times 10^{-4}$ at $Kn = 0.05$ and $\alpha = 0.006$ and $\langle Q \rangle = -0.0818 \times 10^{-4}$ at $Kn = 0.1$ and $\alpha = 0.004$. A comparison of Figs. 5 and 6 shows that when $Kn = 0.0$ there is no back flow, while at $Kn = 0.05$ the back flow occurs at $\alpha = 0.009$ when $t_m = 100$, whereas at $Kn = 0.05$ the back flow occurs at $\alpha = 0.006$ when $t_m = 1000$. Also, at $Kn = 0.1$ the back flow occurs at $\alpha = 0.007$ when $t_m = 100$, whereas at $Kn = 0.05$ the back flow occurs at $\alpha = 0.004$ when $t_m = 1000$. The previous discussion elucidates that the back flow easily occur at low values of α when large values of t_m and Kn are taken into account.

To investigate the behavior of an incompressible ($\chi = 0.0$) Newtonian ($t_m = 0.0$) Maxwellian fluid under the slip effect, the dimensionless net flow rate $\langle Q \rangle$ is plotted versus α in Fig. 7 for $\epsilon = 0.001$, Re $= 10000.0$, $\chi = 0.0$, $t_m = 0.0$, and $Kn = (0.0, 0.05, 0.075$ and $0.1)$. Observe that range of $\langle Q \rangle$ is approximately $1.2507 - 1.0723 \times 10^{-5}$ if $Kn = 0.0$, $1.4863 - 1.1082 \times 10^{-5}$ if $Kn = 0.05$, $1.6505 - 0.6820 \times 10^{-5}$ if $Kn = 0.075$ and $1.8616 - 0.0189 \times 10^{-5}$ if $Kn = 0.1$ for $0.0005 \leq \alpha \leq 0.01$. Furthermore, at low values of α, the net flow $\langle Q \rangle$ increases with increasing Kn and decreases with increasing Kn at high values of α. Moreover, $\langle Q \rangle$ decreases with increasing α and the rate of decrease of $\langle Q \rangle$ increases with an increase in Kn. The behavior of an incompressible ($\chi = 0.0$) non-Newtonian Mexwellian fluid under the slip effects is studied in Fig. 8. In this figure the net flow rate $\langle Q \rangle$ is plotted versus α, for $\epsilon = 0.001$, Re $= 10000.0$, $\chi = 0.6$ and $t_m = 1000.0$ and $Kn = 0.0, 0.05$ and 0.1. Note that $\langle Q \rangle$ decreases with increasing α to a certain value of α and then increases with increasing α. Furthermore, $\langle Q \rangle$ decreases with increasing α and the negative value of $\langle Q \rangle$ for $Kn = 0.05$ begins at $\alpha = 0.004$ and equals

-0.0489×10^{-5}, while the negative value of $\langle Q \rangle$ for $Kn = 0.1$ begins at $\alpha = 0.003$ and equals -0.2146×10^{-5}.

In Fig. 9 the net flow rate $\langle Q \rangle$ is plotted versus α for the following set of parameters: $\epsilon = 0.001$, $\mathrm{Re} = 10000.0, \chi = 0.6$ and $t_m = 10000$ (deeply non-Newtonian regime) and various values of Kn within the range of $0.0 \le \alpha \le 0.01$.Thus figure reveal that in this deeply non-Newtonian regime $\langle Q \rangle$ becomes highly oscillatory and takes negative values for certain values of α. Oscillatory behavior (appearance of numerous maximum in the behavior of a physical value) in the deeply non-Newtonian regime is not new [14]. Further the oscillations at $Kn = 0.0$ are approximately the same as at $Kn \doteq 0.05$ but there is a shift in the value of $\alpha \cong 0.0005$. For example, $\langle Q \rangle = 0.0003 \times 10^{-4}$ when $Kn = 0.0$ and $\alpha = 0.0085$, whereas $\langle Q \rangle = 0.0003 \times 10^{-4}$ when $Kn = 0.05$ and $\alpha = 0.008$. Moreover $\langle Q \rangle$ has the same. approximately, at $Kn = 0.0$ and $Kn = 0.05$ but there is shifting of the value of α.

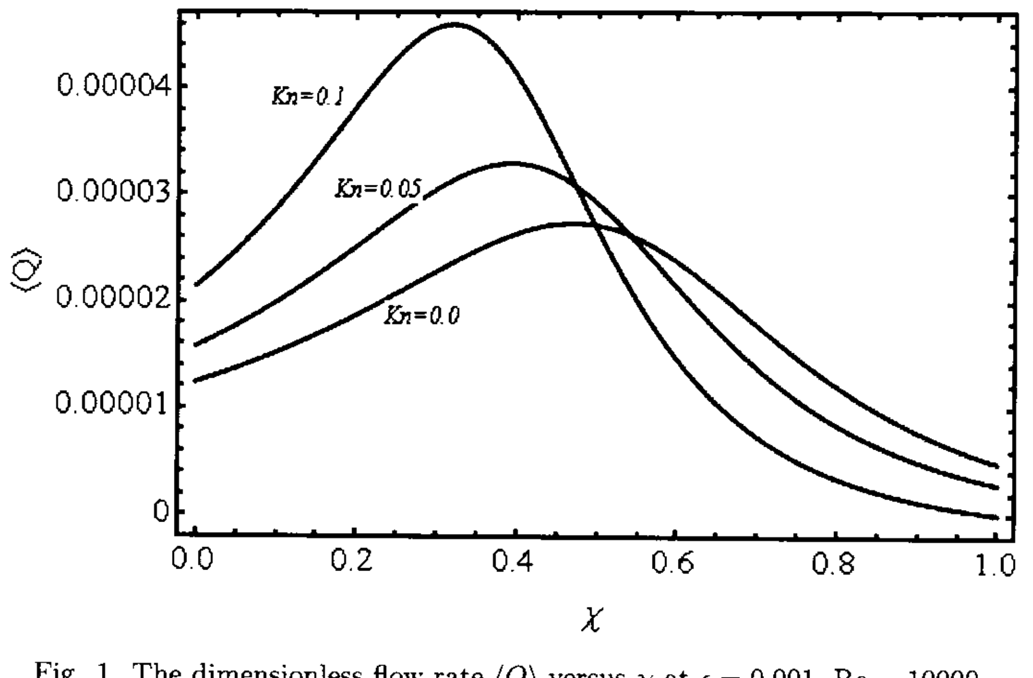

Fig. 1. The dimensionless flow rate $\langle Q \rangle$ versus χ at $\epsilon = 0.001$, $\mathrm{Re} = 10000$, $t_m = 0.0$ and $\alpha = 0.001$

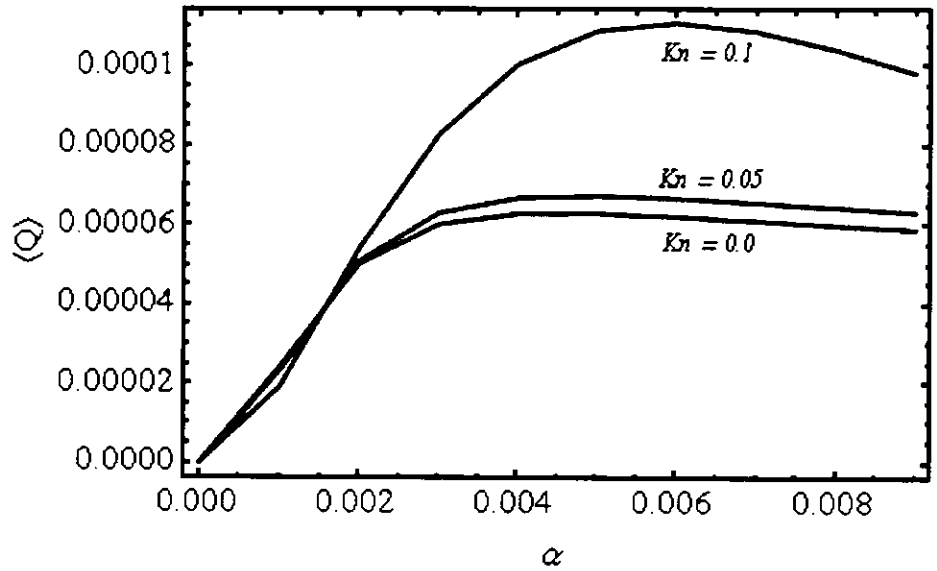

Fig. 2. The dimensionless flow rate $\langle Q\rangle$ versus α at $\epsilon = 0.001$, $\mathrm{Re} = 10000$, $t_m = 0.0$ and $\chi = 0.6$

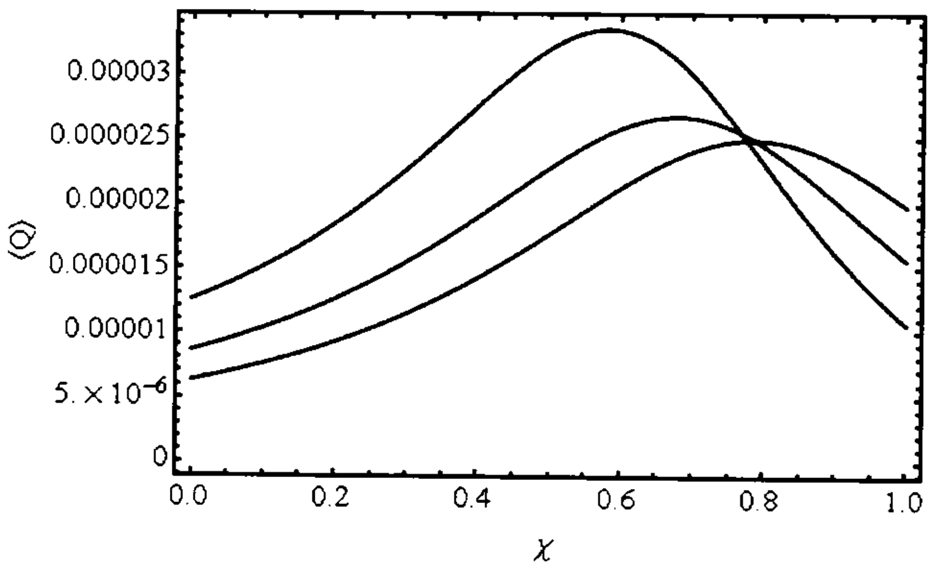

Fig. 3. The dimensionless flow rate $\langle Q\rangle$ versus χ at $\epsilon = 0.001$, $\mathrm{Re} = 10000$, $t_m = 1000$ and $\alpha = 0.001$

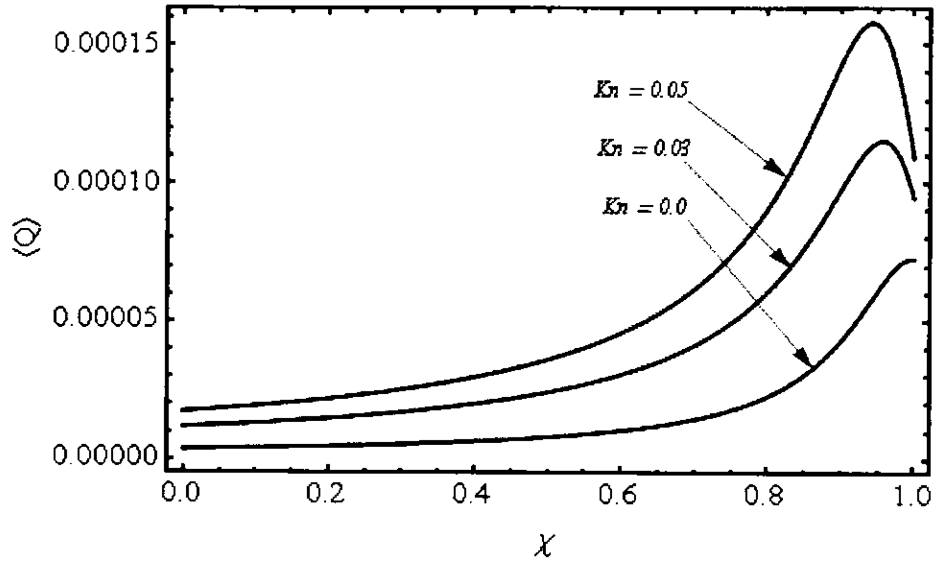

Fig. 4. The dimensionless flow rate $\langle Q \rangle$ versus χ at $\epsilon = 0.001$, Re $= 10000$, $t_m = 10000$ and $\alpha = 0.001$

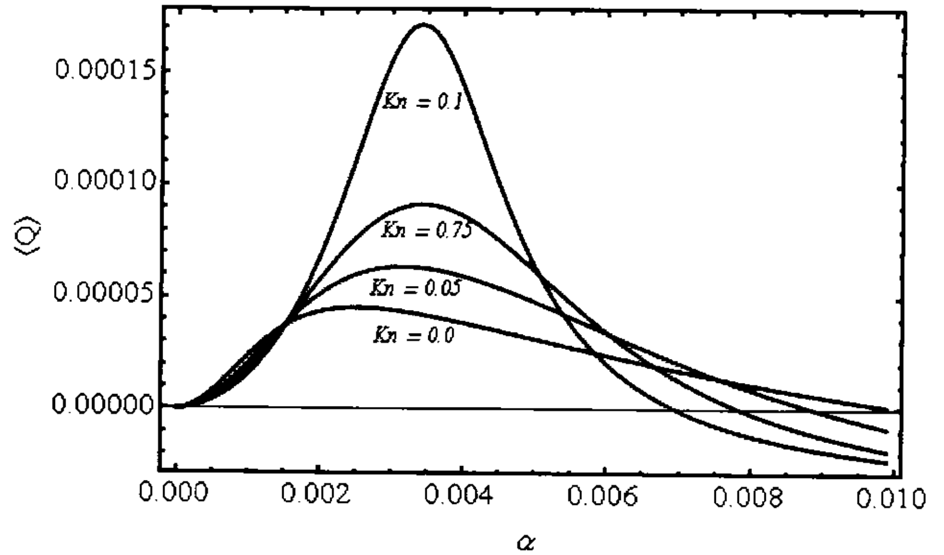

Fig. 5. The dimensionless flow rate $\langle Q \rangle$ versus α at $\epsilon = 0.001$, Re $= 10000$, $t_m = 100$ and $\chi = 0.6$

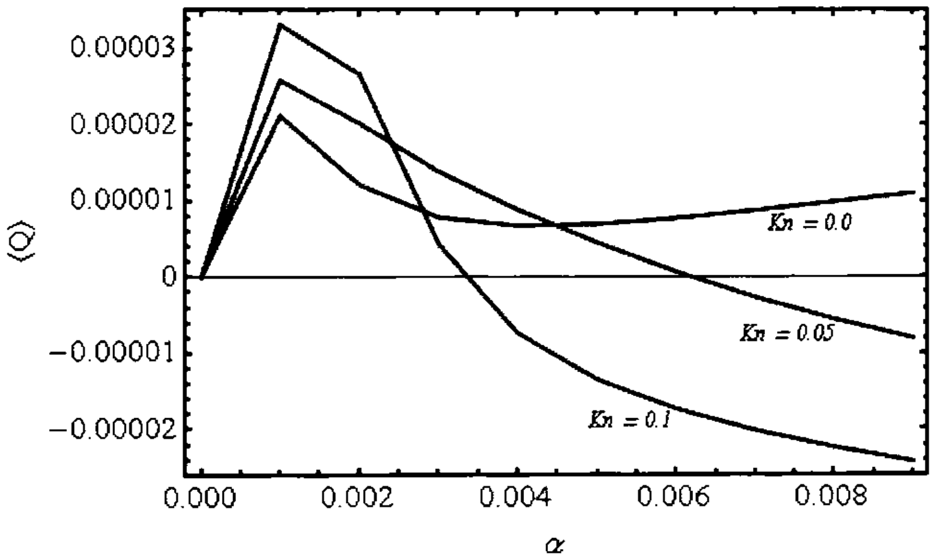

Fig. 6. The dimensionless flow rate $\langle Q \rangle$ versus α at $\epsilon = 0.001$, Re $= 10000$, $t_m = 1000$ and $\chi = 0.6$

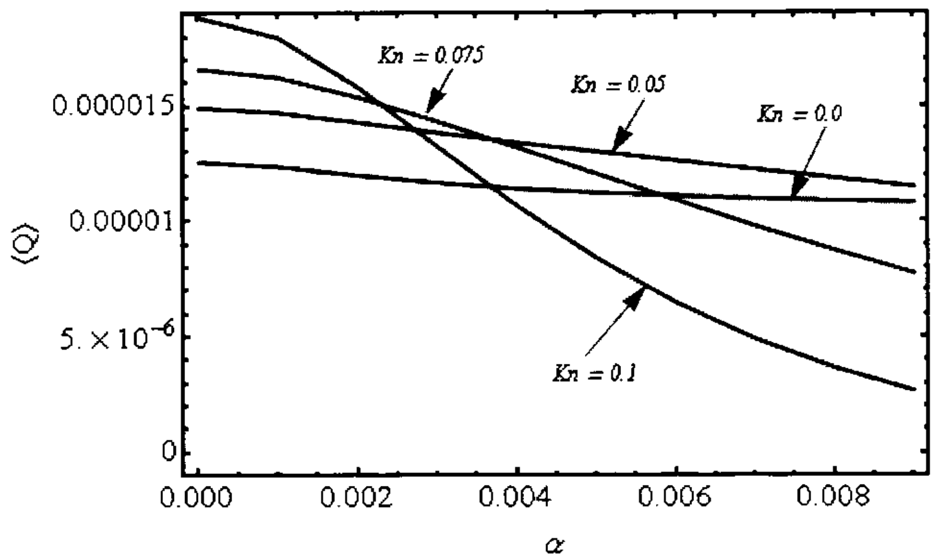

Fig. 7. The dimensionless flow rate $\langle Q \rangle$ versus α at $\epsilon = 0.001$, Re $= 10000$, $t_m = 0.0$ and $\chi = 0.0$

TH- 8616

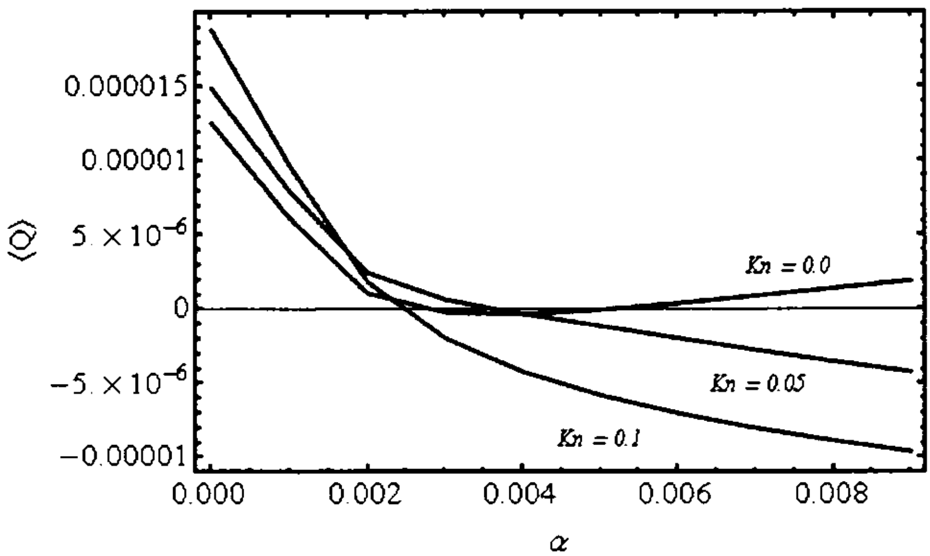

Fig. 8. The dimensionless flow rate $\langle Q\rangle$ versus α at $\epsilon = 0.001$, $\mathrm{Re} = 10000$, $t_m = 1000$ and $\chi = 0.0$

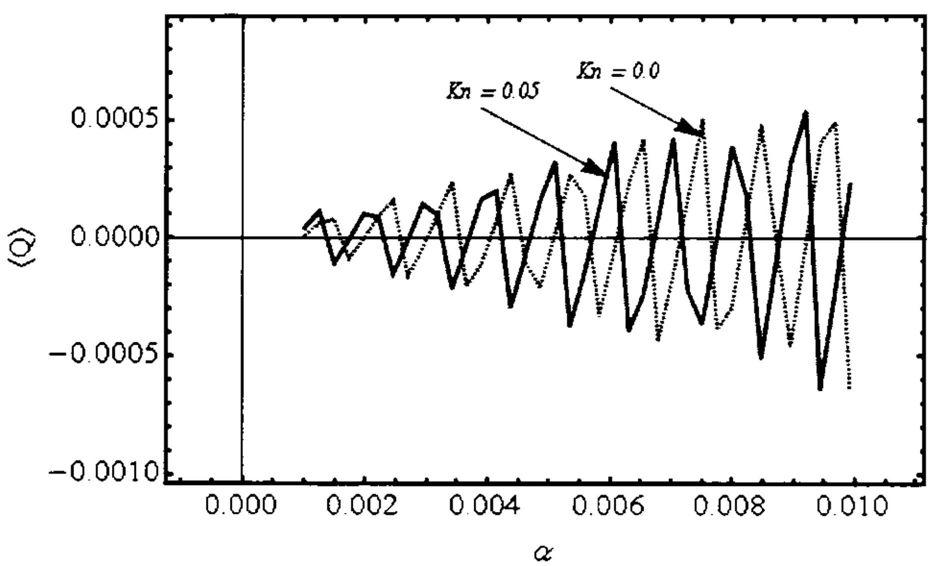

Fig. 9. The dimensionless flow rate $\langle Q\rangle$ versus α at $\epsilon = 0.001$, $\mathrm{Re} = 10000$, $t_m = 10000$ and $\chi = 0.6$

Chapter 3

Slip effects on peristaltic compressible flow of a Jeffrey fluid

This chapter extends the analysis of chapter 2 for a linear Jeffrey fluid model. Jeffrey fluid model includes Newtonian and Maxwell fluid models as a special case. The governing equations involve retardation time as a new parameter which was absent in the equations of chapter 2. The effects of the retardation time on net flow rate are discussed in detail.

3.1 Flow equations

The fundamental equations used in the derivation of the governing equations for the problem considered here are (1.18) and (1.21). We assume a similar geometry as considered in chapter 2. However, the fluid model considered here is the extension of the model used in the chapter 2. It is assumed the properties of the material flowing through cylindrical tube (pore) are described by the constitutive relation of the following form

$$\left(1+t_m\frac{\partial}{\partial t}\right)\mathbf{S}=\mu\left(1+t_r\frac{\partial}{\partial t}\right)\left(\mu\overline{\mathbf{A}}_1-\frac{2}{3}\mu\left(\mathbf{\nabla}.\mathbf{V}\right)\mathbf{I}\right), \tag{3.1}$$

where t_r is the retardation time. Note that if we take $t_r=0$ the fluid model used in chapter 2 is retrieved. Now to obtain the governing equation I apply operator, $\left(1+t_m\frac{\partial}{\partial t}\right)$ on both sides of Eq. (1.21) and eliminate τ in it using Eq. (3.1). Following this I get

$$\left(1+t_m\frac{\partial}{\partial t}\right)\left(\rho\frac{\partial \mathbf{v}}{\partial t}+\rho(\mathbf{v}.\boldsymbol{\nabla})\mathbf{v}\right)=\begin{array}{c}-\left(1+t_m\frac{\partial}{\partial t}\right)\boldsymbol{\nabla}p\\ +\mu\left(1+t_r\frac{\partial}{\partial t}\right)\left(\mu\overline{\mathbf{A}}_1-\frac{2}{3}\mu\left(\boldsymbol{\nabla}.\mathbf{V}\right)\mathbf{I}\right).\end{array}\tag{3.2}$$

Equation (3.2) differs from its counterpart in chapter 2 i.e. Eq. (2.7) due to the presence of t_r in it. It reduces to Eq. (2.7) for $t_r = 0$. This is the only equation which changes in the extended problem and rest of the governing equations and boundary conditions remain same. In component form Eq. (3.2) can be written as

$$\left(1+t_m\frac{\partial}{\partial t}\right)\left[\rho\frac{\partial v_r}{\partial t}+\rho\left(v_r\frac{\partial v_r}{\partial r}+v_z\frac{\partial v_r}{\partial z}\right)\right]=\begin{array}{c}-\left(1+t_m\frac{\partial}{\partial t}\right)\frac{\partial p}{\partial r}+\mu\left(1+t_r\frac{\partial}{\partial t}\right)\left(\frac{\partial^2 v_r}{\partial r^2}+\frac{1}{r}\frac{\partial v_r}{\partial r}-\frac{v_r}{r^2}+\frac{\partial^2 v_r}{\partial z^2}\right)\\ +\frac{\mu}{3}\left(1+t_r\frac{\partial}{\partial t}\right)\frac{\partial}{\partial r}\left(\frac{\partial v_r}{\partial r}+\frac{v_r}{r}+\frac{\partial v_z}{\partial z}\right),\end{array}\tag{3.3}$$

$$\left(1+t_m\frac{\partial}{\partial t}\right)\left[\rho\frac{\partial v_z}{\partial t}+\rho\left(v_r\frac{\partial v_z}{\partial r}+v_z\frac{\partial v_z}{\partial z}\right)\right]=\begin{array}{c}-\left(1+t_m\frac{\partial}{\partial t}\right)\frac{\partial p}{\partial z}+\mu\left(1+t_r\frac{\partial}{\partial t}\right)\left(\frac{\partial^2 v_z}{\partial r^2}+\frac{1}{r}\frac{\partial v_z}{\partial r}+\frac{\partial^2 v_z}{\partial z^2}\right)\\ +\frac{\mu}{3}\left(1+t_r\frac{\partial}{\partial t}\right)\frac{\partial}{\partial z}\left(\frac{\partial v_r}{\partial r}+\frac{v_r}{r}+\frac{\partial v_z}{\partial z}\right),\end{array}\tag{3.4}$$

Thus the problem considered here is governed by Eqs. (2.4), (2.6), (2.8), (3.3) and (3.4). For the sake of convenience of reader these equations in their non-dimensionless form are written as follows

$$\frac{\partial\rho}{\partial t}+v_r\frac{\partial\rho}{\partial r}+v_z\frac{\partial\rho}{\partial z}+\rho\left(\frac{\partial v_r}{\partial r}+\frac{v_r}{r}+\frac{\partial v_z}{\partial z}\right)=0,\tag{3.5}$$

$$\left(1+t_m\frac{\partial}{\partial t}\right)\left[\rho\frac{\partial v_r}{\partial t}+\rho\left(v_r\frac{\partial r}{\partial r}+v_z\frac{\partial r}{\partial z}\right)\right]=\begin{array}{c}-\left(1+t_m\frac{\partial}{\partial t}\right)\frac{\partial p}{\partial r}+\frac{1}{\mathrm{Re}}\left(1+t_r\frac{\partial}{\partial t}\right)\left(\frac{\partial^2 v_r}{\partial r^2}+\frac{1}{r}\frac{\partial v_r}{\partial r}-\frac{v_r}{r^2}+\frac{\partial^2 v_r}{\partial z^2}\right)\\ +\frac{1}{3R_e}\left(1+t_r\frac{\partial}{\partial t}\right)\frac{\partial}{\partial r}\left(\frac{\partial v_r}{\partial r}+\frac{v_r}{r}+\frac{\partial v_z}{\partial z}\right).\end{array}\tag{3.6}$$

$$\left(1+t_m\frac{\partial}{\partial t}\right)\left[\rho\frac{\partial vz}{\partial t}+\rho\left(v_r\frac{\partial z}{\partial r}+v_z\frac{\partial z}{\partial z}\right)\right]=\begin{array}{c}-\left(1+t_m\frac{\partial}{\partial t}\right)\frac{\partial p}{\partial z}+\frac{1}{\mathrm{Re}}\left(1+t_r\frac{\partial}{\partial t}\right)\left(\frac{\partial^2 v_z}{\partial r^2}+\frac{1}{r}\frac{\partial v_z}{\partial r}+\frac{\partial^2 v_z}{\partial z^2}\right)\\ +\frac{1}{3R_e}\left(1+t_r\frac{\partial}{\partial t}\right)\frac{\partial}{\partial z}\left(\frac{\partial v_r}{\partial r}+\frac{v_r}{r}+\frac{\partial v_z}{\partial z}\right),\end{array}\tag{3.7}$$

$$\rho=e^{\chi(\rho-\rho_0)},\tag{3.8}$$

$$v_r\left((1+\eta), z, t\right) = \frac{\partial \eta(z,t)}{\partial t}, v_z\left((1+\eta), z, t\right) = Kn\frac{\partial v_z(r,z,t)}{\partial r}, \tag{3.9}$$

where

$$\eta(z,t) = \epsilon \cos \alpha(z-t).$$

3.2 Solution of the problem

In a similar manner as described in chapter 2 the flow quantities are described are expended in power series of ϵ as:

$$\begin{aligned} p &= p_0 + \epsilon p_1(r,z,t) + \epsilon^2 p_2(r,z,t) + ..., \\ v_r &= \epsilon u_1(r,z,t) + \epsilon^2 u_2(r,z,t) + ..., \\ v_z &= \epsilon v_1(r,z,t) + \epsilon^2 v_2(r,z,t) + ..., \\ \rho &= 1 + \epsilon \rho_1(r,z,t) + \epsilon^2 \rho_2(r,z,t) + ... \end{aligned} \tag{3.10}$$

Upon making use of (3.10) in (3.5) – (3.9), we get following systems:

System of order ϵ :

$$\left(1+t_m\frac{\partial}{\partial t}\right)\frac{\partial u_1}{\partial t} = \begin{array}{l} -\left(1+t_m\frac{\partial}{\partial t}\right)\frac{\partial p_1}{\partial r} + \frac{1}{\mathrm{Re}}\left(1+t_r\frac{\partial}{\partial t}\right)\left(\frac{\partial^2 u_1}{\partial r^2} + \frac{1}{r}\frac{\partial u_1}{\partial r} - \frac{u_1}{r^2} + \frac{\partial^2 u_1}{\partial z^2}\right) \\ +\frac{1}{3R_e}\left(1+t_r\frac{\partial}{\partial t}\right)\frac{\partial}{\partial r}\left(\frac{\partial u_1}{\partial r} + \frac{u_1}{r} + \frac{\partial v_1}{\partial z}\right), \end{array} \tag{3.11}$$

$$\left(1+t_m\frac{\partial}{\partial t}\right)\frac{\partial v_1}{\partial t} = \begin{array}{l} -\left(1+t_m\frac{\partial}{\partial t}\right)\frac{\partial p_1}{\partial z} + \frac{1}{\mathrm{Re}}\left(1+t_r\frac{\partial}{\partial t}\right)\left(\frac{\partial^2 v_1}{\partial r^2} + \frac{1}{r}\frac{\partial v_1}{\partial r} + \frac{\partial^2 v_1}{\partial z^2}\right) \\ +\frac{1}{3R_e}\left(1+t_r\frac{\partial}{\partial t}\right)\frac{\partial}{\partial z}\left(\frac{\partial u_1}{\partial r} + \frac{u_1}{r} + \frac{\partial v_1}{\partial z}\right), \end{array} \tag{3.12}$$

$$\frac{\partial \rho_1}{\partial t} + \frac{\partial u_1}{\partial r} + \frac{u_1}{r} + \frac{\partial v_1}{\partial z} = 0, \tag{3.13}$$

$$\rho_1 = \chi p_1. \tag{3.14}$$

System of order ϵ^2 :

$$\begin{aligned}&\left(1 + t_m\frac{\partial}{\partial t}\right)\left\{\frac{\partial u_2}{\partial t} + \rho_1\frac{\partial u_1}{\partial t} + u_1\frac{\partial u_1}{\partial r} + v_1\frac{\partial u_1}{\partial z}\right\} = -\left(1 + t_m\frac{\partial}{\partial t}\right)\frac{\partial p_2}{\partial r}\\ &+\frac{1}{\mathrm{Re}}\left(1 + t_r\frac{\partial}{\partial t}\right)\left(\frac{\partial^2 u_2}{\partial r^2} + \frac{1}{r}\frac{\partial u_2}{\partial r} - \frac{u_2}{r^2} + \frac{\partial^2 u_2}{\partial z^2}\right) + \frac{1}{3R_e}\left(1 + t_r\frac{\partial}{\partial t}\right)\frac{\partial}{\partial r}\left(\frac{\partial u_2}{\partial r} + \frac{u_2}{r} + \frac{\partial v_2}{\partial z}\right),\end{aligned} \tag{3.15}$$

$$\begin{aligned}\left(1 + t_m\frac{\partial}{\partial t}\right)\left(\frac{\partial v_2}{\partial t} + \rho_1\frac{\partial v_1}{\partial t} + u_1\frac{\partial v_1}{\partial r} + v_1\frac{\partial v_1}{\partial z}\right) = &-\left(1 + t_m\frac{\partial}{\partial t}\right)\frac{\partial p_2}{\partial z} + \frac{1}{\mathrm{Re}}\left(1 + t_r\frac{\partial}{\partial t}\right)\left(\frac{\partial^2 v_2}{\partial r^2} + \frac{1}{r}\frac{\partial v_2}{\partial r} + \frac{\partial^2 v_2}{\partial z^2}\right)\\ &+\frac{1}{3R_e}\left(1 + t_r\frac{\partial}{\partial t}\right)\frac{\partial}{\partial z}\left(\frac{\partial u_2}{\partial r} + \frac{u_2}{r} + \frac{\partial v_2}{\partial z}\right),\end{aligned} \tag{3.16}$$

$$\frac{\partial \rho_2}{\partial t} + u_1\frac{\partial \rho_1}{\partial r} + v_1\frac{\partial \rho_1}{\partial z} + \frac{u_2}{r} + \frac{\partial u_2}{\partial r} + \frac{\partial v_2}{\partial z} + \rho_1\left(\frac{\partial u_1}{\partial r} + \frac{u_1}{r} + \frac{\partial v_1}{\partial z}\right) = 0. \tag{3.17}$$

$$\rho_2 = \chi p_2 + \frac{1}{2}\chi^2 p_1^2. \tag{3.18}$$

Expanding Eq. (3.9) by Taylor expansion around $r = 1$ and substituting from Eq. (3.10) we get the following boundary conditions:

$$u_1(1, z, t) = -\frac{\iota\alpha}{2}(e^{\iota\alpha(z-t)} - e^{-\iota\alpha(z-t)}), \tag{3.19}$$

$$u_2(1, z, t) + \frac{1}{2}(e^{\iota\alpha(z-t)} - e^{-\iota\alpha(z-t)})\frac{\partial u_1}{\partial r}(1, z, t) = 0, \tag{3.20}$$

$$v_1(1, z, t) = Kn\frac{\partial v_1}{\partial r}(1, z, t), \tag{3.21}$$

$$\begin{aligned}&v_2(1, z, t) + \frac{1}{2}\left(e^{\iota\alpha(z-t)} - e^{-\iota\alpha(z-t)}\right)\frac{\partial v_1}{\partial r}(1, z, t)\\ &= Kn\left[\frac{\partial v_2}{\partial r}(1, z, t) + \frac{1}{2}\left(e^{\iota\alpha(z-t)} - e^{-\iota\alpha(z-t)}\right)\frac{\partial^2 v_1}{\partial r^2}(1, z, t)\right].\end{aligned} \tag{3.22}$$

After this we apply the same procedure as described in chapter 2 and arrive at the following determining equations for U_1, V_1 and P_1.

$$-\iota\alpha\left(1-\iota\alpha t_m\right)U_1 = \begin{array}{c} -\left(1-\iota\alpha t_m\right)P_1' + \frac{(1-\iota\alpha t_r)}{\mathrm{Re}}\left(U_1'' + \frac{U_1'}{r} - \frac{U_1}{r^2} - \alpha^2 U_1\right) \\ +\frac{(1-\iota\alpha t_r)}{3R_e}\frac{d}{dr}\left(U_1' + \frac{U_1}{r} + \iota\alpha V_1\right), \end{array} \tag{3.23}$$

$$-\iota\alpha\left(1-\iota\alpha t_m\right)V_1 = \begin{array}{c} -\iota\alpha\left(1-\iota\alpha t_m\right)P_1 + \frac{(1-\iota\alpha t_r)}{\mathrm{Re}}\left(V_1'' + \frac{V_1'}{r} - \alpha^2 V_1\right) \\ +\frac{\iota\alpha(1-\iota\alpha t_r)}{3R_e}\left(U_1' + \frac{U_1}{r} + \iota\alpha V_1\right), \end{array} \tag{3.24}$$

$$U_1' + \frac{U_1}{r} + \iota\alpha V_1 = \iota\alpha\chi P_1, \tag{3.25}$$

$$U_1(1) = \frac{-\iota\alpha}{2}, \tag{3.26}$$

$$V_1(1) = KnV_1'(1). \tag{3.27}$$

From above equations we get

$$U_1(r) = C_1 I_1(\nu r) + C_2 I_1(\beta r), \tag{3.28}$$

$$V_1(r) = \frac{\iota\alpha C_1}{\nu} I_0(\nu r) + \frac{\iota\beta C_2}{\alpha} I_0(\beta r), \tag{3.29}$$

$$P_1(r) = \frac{C_1\left(\nu^2 - \beta^2\right)}{\gamma\nu} I_0(\nu r). \tag{3.30}$$

where

$$\gamma = \frac{(1-\iota\alpha t_m)}{(1-\iota\alpha t_r)}\mathrm{Re} - \frac{\iota\alpha\chi}{3},\ \beta^2 = \alpha^2 - \iota\alpha\frac{(1-\iota\alpha t_m)}{(1-\iota\alpha t_r)}\mathrm{Re}, \tag{3.31}$$

$$\nu^2 = \alpha^2\frac{(1-\chi)\frac{(1-\iota\alpha t_m)}{(1-\iota\alpha t_r)}\mathrm{Re} - (4/3)\,\iota\alpha\chi}{\frac{(1-\iota\alpha t_m)}{(1-\iota\alpha t_r)}\mathrm{Re} - (4/3)\,\iota\alpha\chi}. \tag{3.32}$$

and C_1^* and C_2^* are given as:

$$C_1^* = \frac{\iota\alpha\beta\nu\left[I_0(\beta) - \beta KnI_1(\beta)\right]}{2\left[\alpha^2 I_1(\beta)I_0(\nu) - \beta\nu I_0(\beta)I_1(\nu) + \nu KnI_1(\beta)I_1(\nu)\left(\beta^2 - \alpha^2\right)\right]}, \tag{3.33}$$

$$C_2^* = \frac{-\iota\alpha^3\left[I_0(\nu) - \nu KnI_1(\nu)\right]}{2\left[\alpha^2 I_1(\beta)I_0(\nu) - \beta\nu I_0(\beta)I_1(\nu) + \nu KnI_1(\beta)I_1(\nu)\left(\beta^2 - \alpha^2\right)\right]}. \tag{3.34}$$

Similarly the determining equations for U_{20}, V_{20}, P_{20} and D_{20} read:

$$D_{20} = \chi P_{20} + \chi^2 P_1\overline{P_1}, \tag{3.35}$$

$$U_{20}' + \frac{U_{20}}{r} = -\chi\left(P_1\overline{U_1'} + \overline{P_1}U_1' + \frac{P_1\overline{U_1}}{r} + \frac{\overline{P_1}U_1}{r} + \overline{P_1'}U_1 + P_1'\overline{U_1}\right), \tag{3.36}$$

$$\iota\alpha\chi P_1\overline{U_1} - \iota\alpha\chi\overline{P_1}U_1 + U_1\overline{U_1'} + U_1'\overline{U_1} + \iota\alpha\overline{V_1}U_1 - \iota\alpha V_1\overline{U_1} = \begin{array}{c} -P_{20}' + \frac{1}{\mathrm{Re}}\left(U_{20}' + \frac{U_{20}'}{r} - \frac{U_{20}}{r^2}\right) \\ + \frac{1}{3R_e}\frac{d}{dr}\left(U_{20}' + \frac{U_{20}}{r}\right), \end{array} \tag{3.37}$$

$$\iota\alpha\chi P_1\overline{V_1} - \iota\alpha\chi\overline{P_1}V_1 + U_1\overline{V_1} + \overline{U_1}V_1 = \frac{1}{\mathrm{Re}}\left(V_{20} + \frac{V_{20}}{r}\right), \tag{3.38}$$

$$U_{20}(1) + \frac{1}{2}\left(\overline{U_1'}(1) + U_1'(1)\right) = 0, \tag{3.39}$$

$$V_2(1) + \frac{1}{2}\left(\overline{V_1}(1) + V_1(1)\right) = Kn\left(V_{20}(1) + \frac{1}{2}V_1(1) + \frac{1}{2}\overline{V_1}(1)\right). \tag{3.40}$$

Solving Eqs. (3.35) – (3.40) we get the following expressions.

$$U_{20}(r) = \frac{D_1^*}{r} - \chi\left[P_1(r)\overline{U_1}(r) + \overline{P_1}(r)U_1(r)\right], \tag{3.41}$$

$$V_{20}(r) = D_2^* - \mathrm{Re}\int_r^1 \left[V_1(\tau)\overline{U_1}(\tau) + \overline{V_1}(\tau)U_1(\tau)\right] d\tau. \tag{3.42}$$

In which D_1^* and D_2^* are given by

$$D_1^* = \frac{\iota\alpha Kn}{2}\left(\iota\alpha C_1 I_1(\nu) + \frac{\iota\beta^2 C_2}{\alpha} I_1(\beta) + \iota\alpha\overline{C_1} I_1(\overline{\nu}) + \frac{\iota\overline{\beta}^2\overline{C_2}}{\alpha} I_1(\overline{\beta})\right), \tag{3.43}$$

$$D_2^* = -\frac{1}{2}\left(\overline{V_1'}(1) + V_1'(1)\right) + Kn\left(V_{20}'(1) + \frac{1}{2}V_1''(1) + \frac{1}{2}\overline{V_1''}(1)\right). \tag{3.44}$$

where the values of $V_{20}'(1)$ and $V_1''(1)$ are defined by

$$V_1'(1) = \iota\alpha C_1\left[\nu I_0(\nu) - I_1(\nu)\right] + \frac{\iota\beta^2 C_2}{\alpha}\left[\beta I_0(\beta) - I_1(\beta)\right]. \tag{3.45}$$

$$V_{20}'(1) = \mathrm{Re}\left[\begin{array}{l} \frac{i\alpha C_1\overline{C_1}}{\upsilon} I_0(\nu) I_1(\overline{\nu}) + \frac{i\alpha C_1\overline{C_2}}{\upsilon} I_0(\nu) I_1(\overline{\beta}) + \frac{i\beta C_2\overline{C_1}}{\alpha} I_0(\beta) I_1(\overline{\nu}) \\ +\frac{i\beta C_2\overline{C_2}}{\alpha} I_0(\beta) I_1(\overline{\beta}) - \frac{i\alpha C_1\overline{C_1}}{\overline{\upsilon}} I_0(\overline{\nu}) I_1(\nu) - \frac{i\alpha C_2\overline{C_1}}{\overline{\upsilon}} I_0(\overline{\nu}) I_1(\beta) \\ -\frac{i\overline{\beta} C_1\overline{C_2}}{\alpha} I_0(\overline{\beta}) I_1(\nu) - \frac{i\overline{\beta} C_2\overline{C_2}}{\alpha} I_0(\overline{\beta}) I_1(\beta) \end{array}\right]. \tag{3.46}$$

The net flow rate is given by the following integral

$$\langle Q\rangle = 2\pi\epsilon^2 \int_0^1 V_{20}(r) r dr. \tag{3.47}$$

3.3 Discussion

The primary objective of this study is to analyze the effects of t_r on the net flow rate $\langle Q\rangle$. To investigate the behavior of $\langle Q\rangle$ in presence of t_r I have plotted Figures (3.1) – (3.9). In Fig. 3.1 the net flow rate $\langle Q\rangle$ is plotted against χ for various values of t_r for relatively small values of t_m i.e. $t_m = 1000$. It is observed from this figure that $\langle Q\rangle$ increases attains maximum and then decreases by increasing χ. This maximum is lowest for a Maxwell fluid and greatest for a Jeffrey fluid. The maximum for Newtonian fluid lies in between.

Figure 3.2 elucidates the behavior of $\langle Q\rangle$ of various values of t_r and non-zero values of Kn i.e. $Kn = 0.05$. This figure give similar result as observed in Fig. 3.1. However, a closer look at Fig. 3.1 and 3.2 reveals that $\langle Q\rangle$ attains a greater maximum for $Kn = 0.05$. Thus the slip at the wall enhances the magnitude of $\langle Q\rangle$.

Figure 3.3 shows the variation of net flow rate $\langle Q\rangle$ against χ for various values of t_r in deeply non-Newtonian regime i.e. for $t_m = 10000$. Note that for a Maxwell the net flow rate increases monotonically and there is no appearance of maxima in values of $\langle Q \rangle$. But for Newtonian and Jeffrey fluid $\langle Q \rangle$ increases, attains a maximum and then decreases by increasing χ. Thus a Jeffrey fluid behaves differently from Maxwell fluid in deeply non-Newtonian regime. Figure 3.4 is prepared to see the variation of $\langle Q \rangle$ in in deeply non-Newtonian regime for non-zero values of Kn $(= 0.05)$. This figure reveals the similar results as seen through Fig. 3.3. Figure 3.5 illustrates the variation of $\langle Q \rangle$ versus dimensionless tube radius α for different values of t_r and $Kn = 0$. It is noted from this figure that for a Maxwell fluid $\langle Q \rangle$ increases by increasing α, reaches a maximum and then decreases to zero. However, for Jeffrey fluid $\langle Q \rangle$ does not become zero over the considered range of α. Further for a Newtonian fluid it increases by increasing α and then become nearly independent of α. The observation of Figure 3.5 are in the regime where non-Newtonian effects are not prominent and $Kn = 0$. When $Kn = 0.05$ and $t_m = 100$, the net flow rate in case of Newtonian fluid is greater than Jeffrey and Maxwell fluid which is evident from Figure 3.6. Moreover, due to the presence of slip $\langle Q \rangle$ first increases, reaches a maximum and then decreases by increasing α for all three fluids (Jeffrey, Maxwell and Newtonian). Figure 3.7 gives similar results as observed through Figure 3.6. Interestingly for $Kn = 0.05$ and $t_m = 1000$ the behavior of $\langle Q \rangle$ is somewhat different. Here its maximum value is lowest for Maxwell fluid and highest for Jeffrey fluid (Figure 3.8).

Figure 3.9 presents the variation of $\langle Q \rangle$ plotted against α for various values of $t_r = 10000$ (non-Newtonian regime). This figure depicts that $\langle Q \rangle$ is highly oscillatory for a Maxwell fluid and attains negative values. The negative values of $\langle Q \rangle$ mean the presence of back flow i.e. flow in the opposite direction of propagation of peristaltic wave. However, the oscillatory behavior of $\langle Q \rangle$ decreases and it become positive for large values of t_r.

From the above discussion the following important conclusions can be drawn.

- The net flow rate $\langle Q \rangle$ when plotted against χ attains a higher maximum for a Jeffrey fluid in comparison with Maxwell and Newtonian fluid in a viscous regime (regime where viscous effects are dominant) for zero as well as non-zero values of Kn. Moreover, maximum value of $\langle Q \rangle$ for a Newtonian fluid is higher than the Maxwell fluid.

- In extreme non-Newtonian regime the graph of $\langle Q \rangle$ versus χ still attains a higher maximum for Jeffrey fluid in comparison with Maxwell and Newtonian fluid. However, the maximum value of $\langle Q \rangle$ for Maxwell fluid is higher than that of Newtonian fluid.

- The net flow rate when plotted against α attains higher values for a Newtonian fluid in comparison with Jeffrey and Maxwell fluid for small values of t_m ($t_m = 100$) and $Kn = 0, 0.05$. Similar is the case when $t_m = 1000$ and $Kn = 0$. However, when $t_m = 1000$ and $Kn = 0.05$, $\langle Q \rangle$ attains higher values for a Jeffrey fluid in comparison with Maxwell and Newtonian fluid.

- Finally, in extreme non-Newtonian regime the results also reveal that the back flow and oscillation in $\langle Q \rangle$ are suppressed for Jeffrey fluid in comparison with Maxwell fluid whether Kn is zero or non-zero.

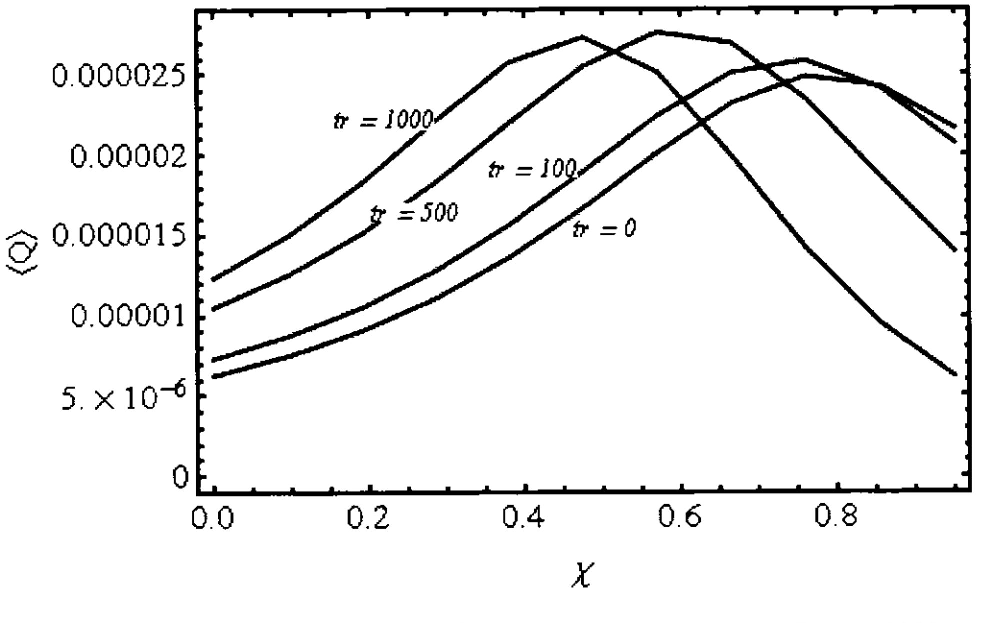

Fig.1. The dimensionless flow rate $\langle Q \rangle$ versus χ at $\epsilon = 0.001$, Re $= 10000$, $t_m = 1000$, $\alpha = 0.001$ and $Kn = 0.0$

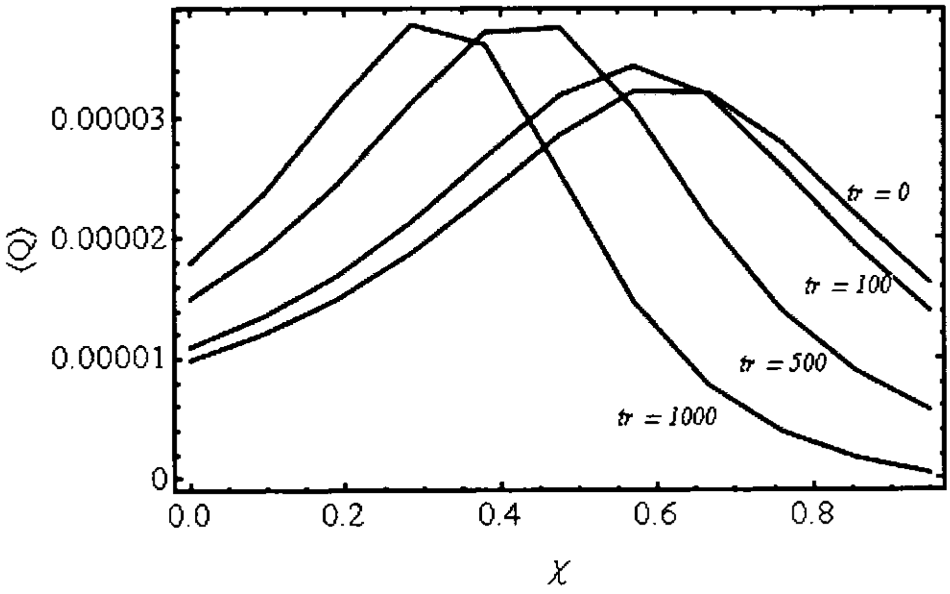

Fig.2. The dimensionless flow rate $\langle Q \rangle$ versus χ at $\epsilon = 0.001$, Re $= 10000$, $t_m = 1000$, $\alpha = 0.001$ and $Kn = 0.05$

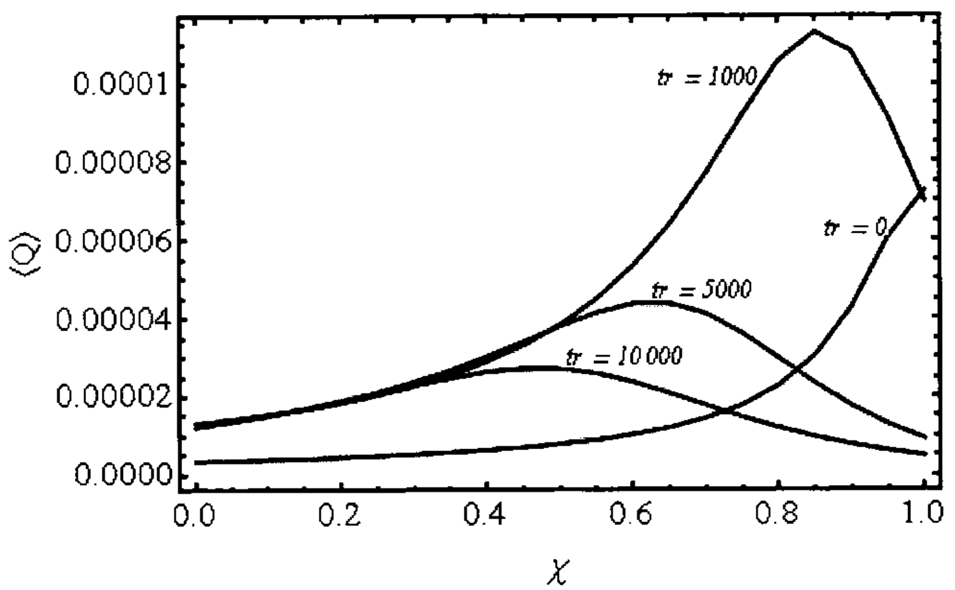

Fig. 3. The dimensionless flow rate $\langle Q \rangle$ versus χ at $\epsilon = 0.001$, Re $= 10000$, $t_m = 10000$, $\alpha = 0.001$ and $Kn = 0.0$

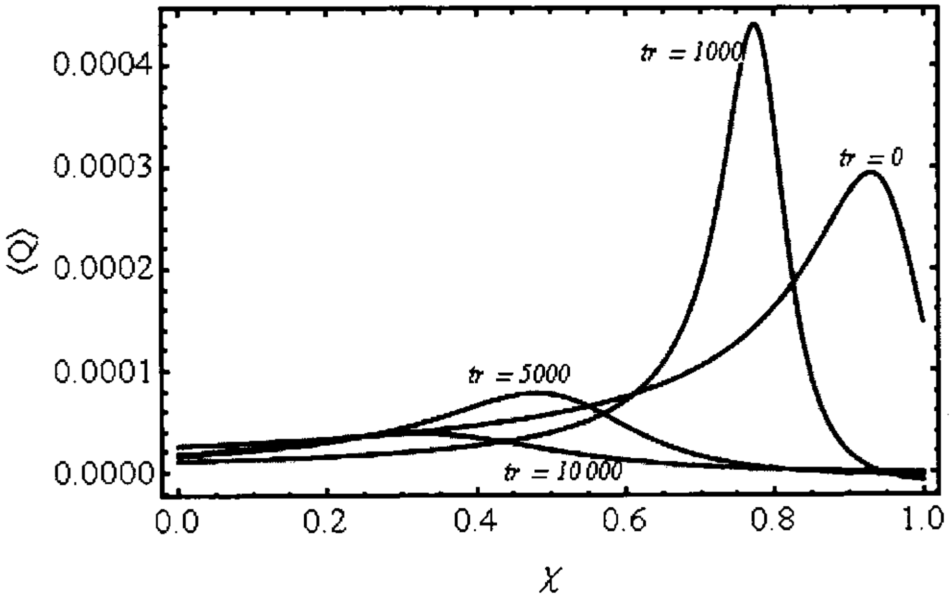

Fig. 4. The dimensionless flow rate $\langle Q \rangle$ versus χ at $\epsilon = 0.001$, $\mathrm{Re} = 10000$, $t_m = 10000$, $\alpha = 0.001$ and $Kn = 0.05$

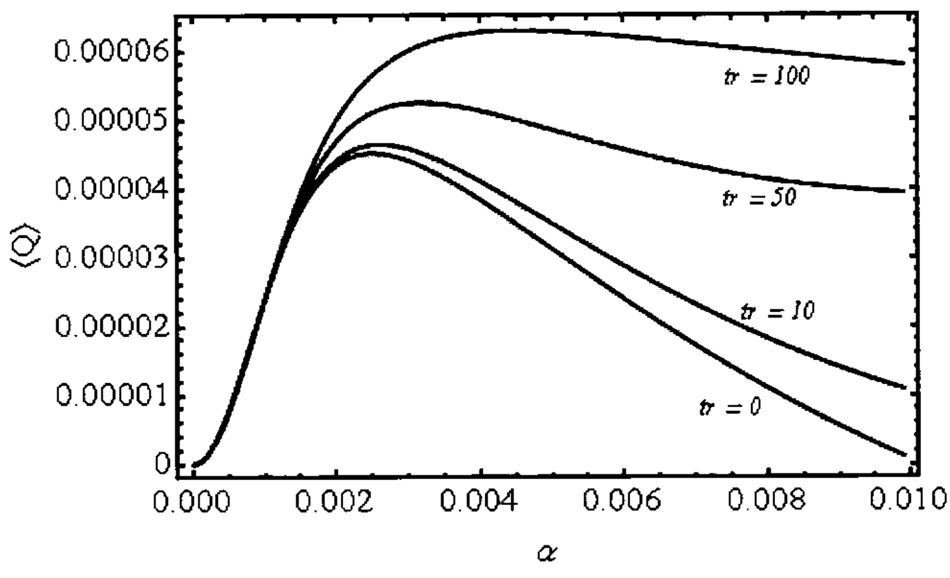

Fig. 5. The dimensionless flow rate $\langle Q \rangle$ versus α at $\epsilon = 0.001$, $\mathrm{Re} = 10000$, $t_m = 100$, $\chi = 0.6$ and $Kn = 0.0$

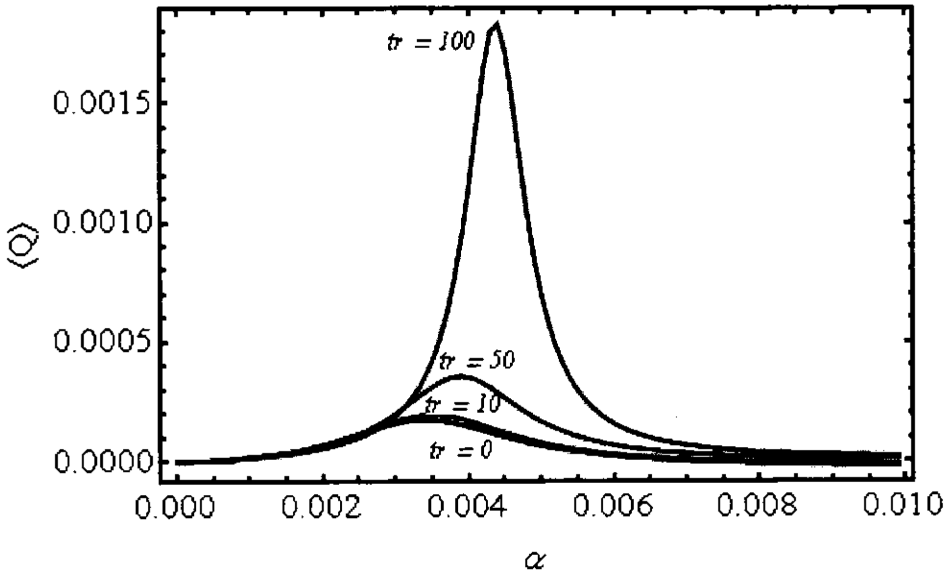

Fig. 6. The dimensionless flow rate $\langle Q \rangle$ versus α at $\epsilon = 0.001$, Re $= 10000$, $t_m = 100$, $\chi = 0.6$ and $Kn = 0.05$

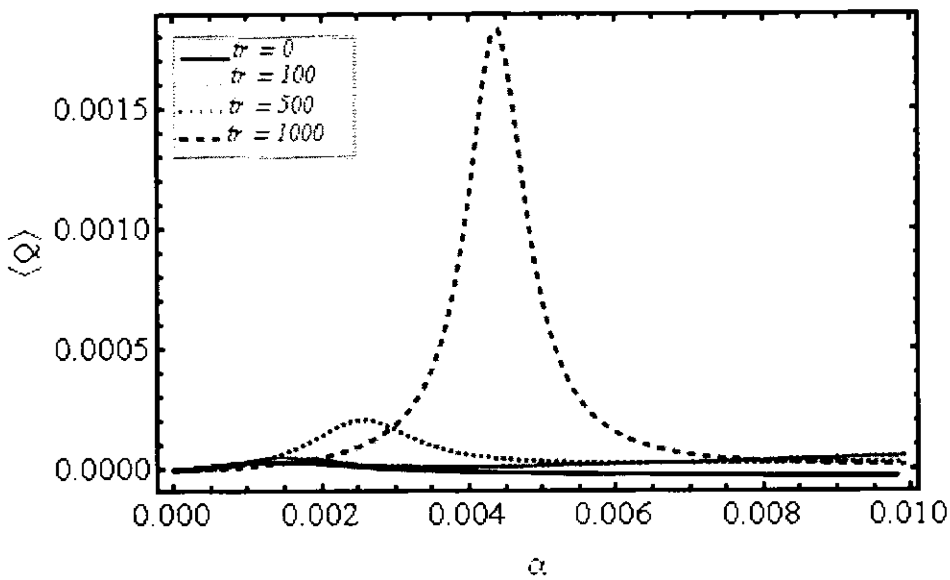

Fig. 7. The dimensionless flow rate $\langle Q \rangle$ versus α at $\epsilon = 0.001$, Re $= 10000$, $t_m = 1000$, $\chi = 0.6$ and $Kn = 0.0$

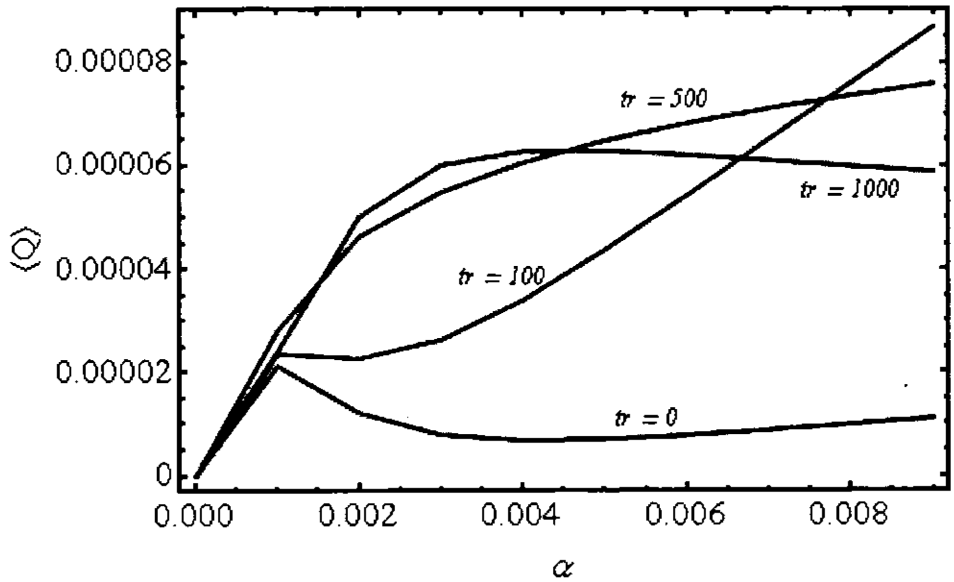

Fig. 8. The dimensionless flow rate $\langle Q \rangle$ versus α at $\epsilon = 0.001$, $\mathrm{Re} = 10000$, $t_m = 1000$, $\chi = 0.6$ and $Kn = 0.05$

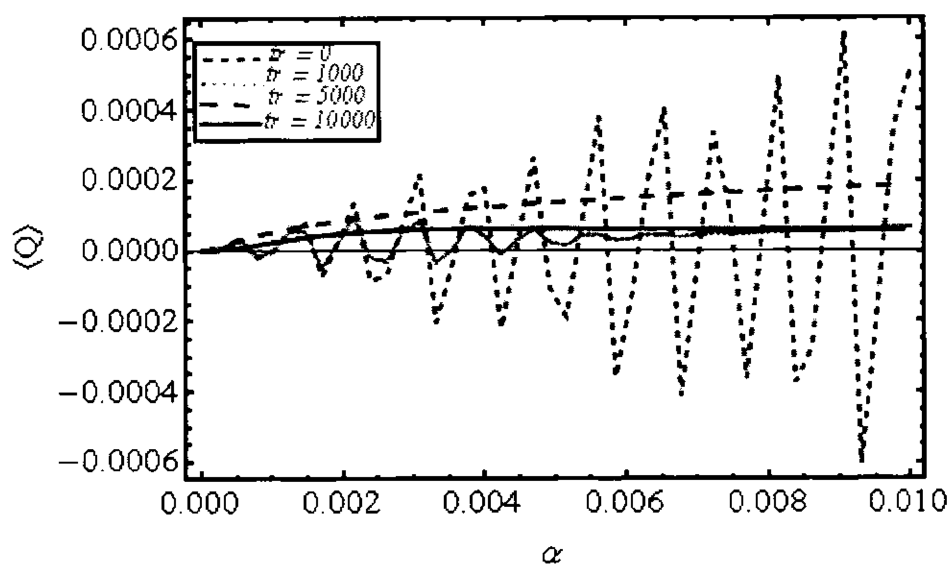

Fig. 9. The dimensionless flow rate $\langle Q \rangle$ versus α at $\epsilon = 0.001$, $\mathrm{Re} = 10000$, $t_m = 10000$, $\chi = 0.6$ and $Kn = 0.0$

Bibliography

[1] A. M. Siddiqui and W.H. Schwarz, Peristaltic pumping of a third order fluid in a planer channel. Rheol. Acta **32**, 47 – 56 (1993).

[2] A. M. Siddiqui, A. Provost and W. H. Schwarz. Peristaltic flow of a second order fluid in tubes. J. Non-Newtonian Fluid Mech. **53**, 257 – 284 (1994).

[3] T. Hayat, Y. Wang, A. M. Siddiqui, K. Hutter, and S. Asghar, Peristaltic transport of a third order fluid in a circular cylindrical tube, Math. Models and Methods in Appl. Sci. **12**, 1691 – 1706 (2002).

[4] T. Hayat, Y. Wang, A. M. Siddiqui and K. Hutter, Peristaltic motion of Johnson-Segalman fluid in a planar channel. Math. Problems. Eng. **1**, 1 – 23 (2003).

[5] Abd El Hakeem Abd El Naby, A.E.M. El Misery, M.F. Abd El Kareem, Effects of a magnetic field on trapping through peristaltic motion for generalized Newtonian fluid in channel. Physica A **367**, 79 – 92 (2006).

[6] M. H. Haroun, Effect of Deborah number and phase difference on peristaltic transport of a third-order fluid in an asymmetric channel. Comm. Non-linear Sci. Numer. Simm. **8**, 1464 – 1480 (2007).

[7] M.V. Subba Reddy, A. Ramachandra Rao, S. Sreenadh Peristaltic motion of a power-law fluid in an asymmetric channel. Int. J. Non-Linear Mech. **42**, 1153 – 1161 (2007).

[8] Y. Wang, T. Hayat and K. Hutter, Peristaltic flow of a Johnson-Segalman fluid through a deformable tube. Theor. Comput. Fluid Dyn. **21**,369 – 380 (2007).

[9] N. Ali, Y. Wang, T. Hayat and M. Oberlack, Long wavelength approximation to peristaltic motion of an Oldroyd 4-constant fluid in a planar channel, Biorheology **45**, 611−628 (2008)

[10] N. Ali, Y. Wang, T. Hayat and M. Oberlack, Numerical solution of peristaltic transport of an Oldroyd 8-constant fluid in a circular cylindrical tube. Cand. J. Phys. **87**, 1047 − 1058 (2009).

[11] A. C. T. Aarts and G. Ooms, Net flow of compressible viscous liquids induced by travelling waves in porousmedia. Engineering Mathematics **34**, 435 − 450 (1998).

[12] R. D. Duhon, An Investigation of the Effect of Ultrasonic Energy on the Flow of Fluids in Porous Media. Ph.D. thesis, University of Oklahoma (1964).

[13] R. F. Ganiev, L. E. Ukrainskii and K. V. Frolov, Wave mechanism for the acceleration of a liquid flowing in capillaries and porous media. Sov. Phys. Dokl. **34**, 519 − 521 (1989).

[14] D. Tsiklauri and I. Beresnev, Non-Newtonian effects in the peristaltic flow of a Maxwell fluid. Physical review E. **64**, 036303 (2001).

[15] E. F. El-Shehawy, N. T. El-Dabe and I. M. El-Desoky, Slip effects on the peristaltic flow of a non-Newtonian Maxwellian fluid. Acta Mechanica **186**, 141 − 159 (2006).

[16] T. Hayat, N. Ali, and S. Asghar, An analysis of peristaltic transport for flow of a Jeffrey fluid. Acta Mechanica **193**, 101 − 112 (2007).

[17] Chu, W, Stokes slip flow between corrugated walls. ZAMP **47**, 591 − 598 (1996).

[18] Yin, F., Fung, Y. C., Peristaltic waves in circular cylindrical tubes. J. App. Mech. **36**, 579 − 587 (1969).

[19] Del Rio, J. A., De Haro, M. L., Whitaker, S., Enhancement in the dynamic response of a viscoelastic fluid flowing in a tube. Phys. Rev. E **58**, 6323 − 6327 (1998).

[20] Vasudeviah, A., Balamurugan, K., Stokes slip flow in a corrugated pipe. Int. J. Engng. Sci. **37**, 1629 − 1641 (1999).

[21] Takabatake, S., Ayukawa, K., Mori, A., Peristaltic pumping in circular cylindrical tubes: a numerical study of fluid transport and its efficiency. J. Fluid Mech. **193**, 267 – 283(1988).

[22] Nayfeh, A. H., Perturbation methods. John Wiley & Sons (1973).